OCEAN APPLICATIONS TECHNICAL NOTE 20.

PREDICTION OF SUMMER TEMPERATURE, RAINFALL AND PRESSURE IN EUROPE FROM PRECEDING WINTER NORTH ATLANTIC OCEAN TEMPERATURE

by

Andrew Colman & Michael Davey.

Met Office
FitzRoy Road, Exeter, Devon. EX1 3PB

ABSTRACT

Statistical prediction of July-August Central England Temperature (CET) from January-February sea surface temperature anomalies (SSTA) in the North Atlantic has been described by Colman (1997). In this paper the method is extended to examine predictability of rainfall, surface temperature and pressure in Europe. Using a January-February North Atlantic SSTA pattern as predictor, it is found that mean, minimum and maximum July-August temperatures over much of North West Europe are predictable using linear regression with correlation skills in the range 0.4 to 0.7, while July-August rainfall and surface pressures are less predictable with correlation up to 0.4. July-August temperatures in SE Canada and NE USA are also predictable with correlation up to 0.3.

The predictability of other seasons and timeescales is also investigated. For UK temperature, half-month to 2-monthly ranges were considered: predictive correlation skills were best for the period mid July to end August. Highest correlations are from predictions of August temperature in eastern France where correlation over 50 years exceeds 0.7. For other seasons, long lead predictability from north Atlantic SSTA was found to be much less than for the summer season.

Analysis of composite cases shows an association of predictable warm summers with movement of anomalously warm SSTA across the North Atlantic from the East coast of the USA to the Northwest European coast during spring months. Predictability of cold summers seems to be related to persistence of anomalously cold SST near or to the east of the UK throughout spring.

Coherence between the winter SST and the summer temperatures is strongest at 7-8 years. Other studies have revealed North Atlantic ocean variability at this timescale.

This is a slightly expanded version of the paper with the same name and authors which has been accepted for publication by I.J.Climatology.

1. INTRODUCTION

On seasonal timescales, anomalous atmospheric conditions are often linked to sea surface temperature anomalies (SSTA). For example, Rowell (1998) discusses analyses of sea level pressure (SLP) and precipitation variability associated with SSTA, and Barnston and Smith (1996) discuss empirical relationships between global scale SST patterns and continental precipitation and temperature anomaly patterns. Other examples include Ratcliffe and Murray, (1970) and Ropelewski and Halpert, (1987).

In some regions, knowledge of preceding SSTA can be used to make seasonal forecasts using empirical and/or dynamical prediction models (see Ward et al. (1993), Folland et al. (1991), Barnston and Smith (1996), reviews by Palmer and Anderson (1994), Hastenrath (1995) and Carson (1998)).

In a previous study by Colman (1997) (C97 hereafter), Central England Temperature (CET) in July-August was found to be linearly related to the strength and sign of a preceding January-February SSTA pattern in the North Atlantic. The SSTA pattern was represented by the leading variance eigenvector, which had a tripole structure with extrema near the east USA coast, south of Greenland (with opposite sign), and near western Europe. The correlation of the timeseries of the January-February eigenvector coefficients with July-August CET exceeded 0.45. This level is sufficient for predictions with significant (but limited) skill to be made, and on that basis experimental statistical long-lead forecasts of CET (Colman & Davey 1996, 1997) have been produced by the UK Meteorological Office (UKMO), using the projection of the eigenvector pattern as a predictor. Investigations of England and Wales rainfall predictability in C97 showed little connection with this SSTA predictor however.

Other studies have found other statistical connections between SSTA and large scale European temperatures and rainfall (Johansson et al. 1998, Barnston 1994, Barnston and Smith 1996). As atmospheric conditions in Europe in general behave similarly on a broad scale, extending to the UK, it is possible that the SSTA predictor used for CET may provide useful forecasts for other European regions and variables. This possibility has been explored, and the results are described in this paper. As well as mean temperatures and rainfall, maximum and minimum temperatures and surface pressures have been investigated.

The various historical datasets are described in section 2. In section 3, predictability of July-August surface temperature, rainfall, and sea level pressure (SLP) across Europe and beyond is investigated. The North Atlantic SSTA predictor is essentially the same as in C97, modified slightly by enlarging the ocean domain from that used in C97. (This extension produces a slight increase in predictive skill.) In section 4, predictability of target periods from 2 weeks to 2 months within the summer season is investigated, firstly for the UK, then for western Europe. Predictability of CET in other seasons is also investigated. In some circumstances a second north Atlantic SSTA predictor can provide useful predictive information. The performance of this second predictor, both alone and combined with the first predictor, is assessed in section 5. In section 6 some insight into the mechanisms behind the predictability is sought by selecting composites of years based on the success and the anomaly sign of the forecasts, and investigating the progression of SSTA and SLP anomalies from the winter through to the summer being predicted.

2. HISTORICAL DATA

2.1 Sea surface temperature

Versions of the Meteorological Office Historical Sea Surface Temperature (MOHSST) dataset have been used. MOHSST version 6B is the same as MOHSST version 6C, but without some gap filling and smoothing at the 5x5 degree resolution (Parker et al., 1996). MOHSST was selected rather than the Meteorological Office's gridded globally complete Global Ice and Sea Surface Temperature (GISST) data (Rayner et al., 1996) because MOHSST contains fewer (none for 6B) datapoints that have been estimated from surrounding values in space and time. Unlike GISST, the MOHSST data are solely sea temperatures and do not include ice data. Using a dataset without missing data estimates also avoids a possible systematic positive bias in skill assessment due to data from later times being used to fill gaps using timewise interpolation.

The predictions described in the following sections use North Atlantic SSTA as the predictor. The anomalies are departures from monthly 1961-1990 climatology. In C97 the predictor pattern was the first variance eigenvector (or empirical orthogonal function (EOF)) of North Atlantic January-February SSTA between 40N and 70N. In this study the ocean domain has been extended to cover 20N to 80N. The leading four EOFs, calculated from January-February anomalies from using 1901 to 1990 MOHSST6C data, are shown in fig. 1. EOF1 (Fig. 1a, associated with 25% of the total variance) is very similar to the pattern used in C97: there is a tripole pattern with (as shown) positive centres in the west and northeast Atlantic and a negative centre in the central Atlantic south of Greenland.

Predictor values were calculated by projecting EOF1 on various SST datasets. Table 1 shows temporal correlations between January-February predictor values and July-August CET (cf C97). The highest correlations (0.52 for 1946-95) were obtained using projections on MOHSST6B data. The same table contains results using EOF1 from a smaller domain (40N-70N, C97) and different datasets. EOF1 from MOHSST6C projected on MOHSST6B gives the best results, but differences from the other combinations are small.

The time series T1 consists of projections of EOF1 on the MOHSST6B data for 1946 to 1995 (fig. 2a, solid line). Note that positive values of T1 correspond to times when the projection of the EOF 1 pattern in fig. 1 is positive; i.e. when SSTA tends to be positive near Europe, negative south of Greenland and positive in the west Atlantic. The relation of T1 to other variables is described in following sections. In C97 the projections of lower order EOFs were found not to improve July-August CET predictions. However, summer rainfall has been found to be correlated with the time series of projections of EOF2 onto MOHSST6B data (T2) (fig. 2b).

2.2 Night marine air temperature

To support the results obtained with SSTA, some analyses were repeated using Night Marine Air Temperature Anomalies (NMATA) (Parker et al., 1995). These 5x5 monthly mean anomalies are compiled from Meteorological Office records in a similar fashion to SSTA and form a dataset called Meteorological Office Historical Marine Air Temperature (MOHMAT4). They are based on air temperature observations on ship decks made at night (daytime observations are biased by solar heating of decks). NMAT provides a measure of how the SSTA relates to the atmosphere and also acts as a check on SSTA.

2.3 Land surface temperature

The Central England Temperature (CET) index considered by C97 consists of monthly temperature from 1659 on, first assembled by Manley (1974), and updated by Parker et al. (1992). Daily values, including maxima and minima, are available from 1772 to present. Daily CET was compiled using stations from the same area as the monthly CET. CET values are calculated as averages of maximum and minimum temperatures. July-August CET values for 1946-1995 are plotted in fig. 2a.

Fifteen-day temperature anomalies for the UK, divided into 10 districts, are produced routinely and used for the monthly prospect produced regularly by UKMO (Harrison, 1995). These indices enable the assessment of predictability on shorter (intra-seasonal) time scales. The district averages were complied using calendar half-month averages (eg. January 1-15, January 16 -31, February 1-15, February 16-28) for a group of representative stations within each district and are available from 1951.

To extend the predictability study to Europe, we make use of a gridded dataset of combined land and sea surface temperature (Jones, 1994). Averages of land and sea temperature have been calculated for 5x5 degree squares worldwide weighted according to the area of land and sea in each square and are available back to 1856. Data from some urban stations are corrected for increasing urbanization in recent years.

2.4 Sea level pressure

The sea level pressure (SLP) data used in these analyses are monthly 5 latitude x 5 longitude gridded averages by Basnett and Parker (1997), available for 1871 to 1994. These data were produced by blending UKMO daily analysis data with data from Australia and USA.

2.5 Rainfall

The rainfall data used are monthly gridded 3.75 latitude x 2.5 longitude averages of land based raingauge observations compiled by Hulme (1995), available for 1900 to 1994. The England and Wales Rainfall (EWR) index, (Gregory et al., 1992), a series of monthly rainfalls from a selection of stations dating back to 1772, was used to assess rainfall predictability from T1,T2 and lower order EOF predictors.

3. JULY-AUGUST PREDICTIONS FOR WESTERN EUROPE

In this section, prediction skills for gridded surface temperature, rainfall and SLP are described. The long-lead predictability has been assessed for western Europe and beyond, using the same method as applied in C97 to investigate CET. While this study is focused on western Europe, predictability beyond this region is also assessed to determine the spatial extent of predictability from the north Atlantic SSTA predictor. With the January-February values of T1 as the predictor, inflated linear regression predictions were made for each year in turn, using the jack-knife technique. (The year to be predicted is excluded from the data when the regression equation is calculated (trained). The two years immediately following the target year were also excluded to minimise any positive bias in skill due to persistence effects. The predicted values were rescaled (inflated) such that the predictions had the same variance as the observations in the relevant training period: this rescaling does not affect correlations.)

The jack-knife predictions were assessed by calculating the temporal anomaly correlation between forecast and observed values for each grid point and variable. The period 1951-94 was selected for assessing predictability because this is the period for which temperature, rainfall and pressure data are all available. Other skill measures have also been applied , eg. terce categories. The correlation skills described here provide a reasonable measure of general prediction skill.

The significance of the correlations was assessed, with serial correlation of predictions and observations taken into account when calculating the degrees of freedom. The significance measures the probability of the calculated correlation if two random indices with the same degrees of freedom were correlated. In most cases serial correlations are too low to imply reduced degrees of freedom so for these cases the number of degrees of freedom is assumed to be the same as the number of years analysed minus 1 (43 for 1951-1994). Correlations significant at the 5% level are referred to as 'significant' in the text below, and the locations of significant correlations are shaded in the figures.

3.1 Surface temperature

Jackknife assessments of mean temperature forecasts revealed an area of significant correlation skill that extends from northwest UK to as far southeast as Croatia and as far northeast as Lithuania (fig. 3a). The highest correlations are in France and southern England with values greater than 0.5. A second but weaker area of significant correlation is located in eastern Canada and NE USA and a weaker still area of reversed sign correlation is in the Eastern Mediterranean.

Jackknife predictions of maximum and minimum temperatures are 5% significantly correlated with observed values over a very similar area of western Europe and N America. The maximum temperature correlations are slightly higher than the minimum temperature equivalents and quite similar to the mean temperature equivalents.

3.2 Pressure

Assessments of jack-knife predictions of SLP (fig. 3b) show areas of significant positive correlation over west-central Europe (max r=0.48) and near Newfoundland, and significant negative correlation around Greenland/Iceland (min r=-0.4). (The actual area of negative correlation near Greenland is smaller than it appears on the figure due to the map projection.)

Thus positive (negative) T1 is associated with anomalously high (low) pressure over Europe and eastern Canada low (high) pressure around Greenland. Geostrophically, this pattern is associated with southwesterly (northeasterly) wind anomalies in the UK region. This tendency is consistent with the temperature anomalies described above: i.e. winds from more temperate latitudes are associated with warmer European temperature.

3.3 Rainfall

The jack-knife predictions of July-August rainfall are significantly negatively correlated with observed values over an area covering much of west-central Europe (fig. 3c) The minimum value is -0.37. Positive (negative) values of T1 are associated with lower (higher) than average rainfall. The area of significant correlation is smaller than for temperature forecasts, with lower correlation values generally (maximum $r < 0.4$). As might be expected, the significant rainfall correlations are closely co-located with the significant SLP correlations. Most of the UK lies outside the region of significant

correlations. This is consistent with C97 which found England and Wales rainfall less predictable than CET.

3.4 1901-1950 Temperature

For earlier years, combined land surface and sea surface temperatures are predictable from the north Atlantic predictor over 1901-50 with correlations up to 0.44 between jack-knife predictions and observed temperatures over western France (fig. 3d). This compares with correlations up to 0.58 with recent 5x5 data (fig. 3a). While the significant correlations for 1901-50 do not extend quite so far south east as the 1951-94 correlations, there is clear predictability of western European summers during the earlier 1901-50 period. Significant correlations are also found in eastern USA and Canada which are also consistent with the 1951-1994 results.

In summary, positive January-February values of the SSTA predictor T1 are significantly associated with warmer temperatures, higher pressure and lower rainfall in July-August over large parts of west-central Europe, and vice-versa. Positive T1 is correlated to a lesser extent with warmer temperature in NE USA and SE Canada.

4. PREDICTABILITY FOR OTHER PERIODS INCLUDING INTRA-SEASONAL PREDICTABILITY

4.1 CET

The results in the last section show that July-August predictability using January-February T1 extends beyond the CET region considered by C97. In this section we first revisit CET to examine predictability for other seasons and for shorter intra-seasonal timescales, using the daily CET data. This gives a more precise estimate of when temperature is predictable. Predictability of all running 2 month CET means using SST EOF1 projections as predictors was assessed using jack-knife linear regression predictions with lead times of 0 to 11 months. The Jackknife correlation skill is displayed as a contour plot (fig. 4). July-August is the only time of year when correlation is clearly significant with values exceeding 0.4.

This assessment for other seasons may be pessimistic, however, as the EOF1 pattern was calculated for January-February conditions. Temperatures in other seasons and for other lead times may be more predictable from different SST patterns.

In this paper we restrict attention to North Atlantic SST. EOFs of North Atlantic SSTA were calculated for the remaining pairs of months in the year, ie. March-April, May-June, July-August, September-October and November-December. Regression equations to predict CET for each month were constructed, using EOF projections for 2 preceding month-pairs as predictors, with a mimimum 2 month lead time. For example, January CET is predicted from July-August and September-October predictors, and April CET is predicted using September-October and November-December predictors.

The first 8 EOFs for each bimonth were considered. Predictors were selected by a "stepwise" technique where predictors 5% significant according to an F test are selected. Predictions for 1946-1995 were made using the jackknife techinque in the same way as the experiments described above. These jackknife predictions differed from the previous predictions in that as well as separate regression equations being calculated for each year, the predictors were selected separately for each year. The correlation scores for each month are plotted in Fig. 5. The highest correlations (greater than 0.3) are for the July and August predictions, which used January-

February T1. Skill for other months is low. The results are similar if CET is substituted with 5x5 degree square mean surface temperatures for NW Europe. For all 5x5 degree squares within the region 55-45N and 10W-10E, skill is higher in summer than in any other season and apart from one marginal exception, significant correlations are confined to summer.

In summary, this study has found significant predictability of UK and nearby temperature from the North Atlantic SSTA patterns to be confined to predicting July-August temperature, using January-February predictor values. Consequently, the remainder of this paper discusses predictability for July and August only.

To assess the shorter time scale predictability, jack-knife linear regression predictions are again made, using Jan-Feb T1 as the predictor. The correlation between predicted and observed CET for 1946-1995 was calculated for continuous periods between June and September of all lengths ranging between 15 days and 4 months. The highest correlation for any continuous daily period is 0.55 for the 52 day period, July 14 - September 3rd. This is slightly higher than the July-August correlation of 0.51. Whilst the difference between these two correlations is small, repeating the analysis over 1901-1945 also showed a higher correlation for July 14- September 3rd than for July and August together (r=0.37 and 0.33 respectively).

4.2 UK Districts

Assessments of predictions of average temperature for the UK divided into 10 regions also showed slightly higher correlations for predictions for 16th July- 31st August than for predictions for the whole of July and August. Predictions of August temperatures were also found to be a little better than July-August predictions. Correlation skill varies with Region. The highest correlations between predicted and observed temperatures occur in the south and east of the UK. For the period 1956-1995 correlations between jack-knife predictions and observations for July 16-August 31 vary from 0.70 for the East Anglian region to 0.59 for Wales and western England to 0.55 for western Scotland (fig. 6). As before, positive (negative) T1 is associated with warmer (colder) summer temperatures. The highest correlations are in the regions closest to the areas with highest SLP correlation (fig. 3c). Warmer temperatures for positive T1 are consistent with pressure anomalies giving warm south or southwesterly wind anomalies, and vice versa in cooler years.

4.3 July and August predictions for Europe

For this study, only monthly data were used for regions beyond the UK. The monthly gridded temperature means were used to assess July and August predictions separately.

Correlations between jack-knife August forecasts and observed values are shown in fig. 7, for mean temperature, rainfall and SLP for 1951-1994 and for mean temperature for 1901-1950. The correlation fields for all 4 variables have similar patterns with higher maxima than the July-August equivalent (fig. 3). Increased correlations occur mainly over the European continent and over SE Canada. August correlation increases over the UK are restricted to a small increase for SLP. The largest correlations are centered over eastern France, where temperature correlations exceed 0.7. This level of correlation skill is similar to that achieved in tropical regions (see e.g. Ward et al., 1993).

Mean August temperatures for 4 stations in Eastern France (Paris, Bourges, Dijon, Nancy) near the correlation maximum (fig. 7a) are plotted against jack-knife predictions for 1951-1995 in fig. 8. The correlation of 0.75 is considerably higher than the CET equivalent

(0.52). On several occasions, the forecast for this area of France was much better than the forecast for UK. For example, in 1974, 1988 and 1992 (years of strong positive T1) the forecasts for England temperatures were much too warm, but temperature anomalies in France were close to those predicted.

A categorical assessment of the Eastern France forecasts for 1951-1995 is shown in table 2a. Three equiprobable categories (terces) are used. Results of separate sets of forecasts for the 4 stations provide a total of 4 x 45 = 180 forecasts. The forecast and observed data were categorised into terces and assessments made over the same 1951-1995 period. Hence the total frequency in each row and column is always 180/3=60. The expected frequency from chance in each of the 9 boxes is 180/9=20. There were 110 correct predictions, compared with an expected (by chance) total of 60, which is clearly significant at the 0.1% level according to a chi square test.

Another feature of the contingency table is its skewed shape. Following an average forecast, warm (terce 3) is observed much more frequently than cold (terce 1), and following a cold (terce 1) forecast, average temperature (terce 2) is observed much more frequently than warm (terce 3). There only two cases of terce 3 being observed following a terce 1 forecast. Similar contingency assessments of predictions for a larger set of western European stations located within the box 10W-20E and 60-40N (an area where correlation is high in fig. 7a) show the same skewness to be evident over much of this region.

Fig. 9 displays the number of cases occurring, station-by-station, for the possibilities (boxes) in the terce contingency table. For most stations there was a skewnesss like that found in table 2 with more warm terce observations than cold terce observations following average forecasts, and there were more average observations following cold forecasts than warm forecasts. This skewness is less visible over the UK. A chi squared test was applied to assess the frequencies for the 57 stations where there is significant correlation between jackknife forecasts and observations for each of the 9 boxes. The frequencies on the cold forecast/cold observed and the warm forecast/ warm observed were significantly (>99.9%) higher than expected by chance, and the frequencies for the cold forecast/warm observed were significantly less than chance (each terce contains 15 cases, so the expected by chance number of cases for each possibility is 5). The variance of the frequencies for the stations within each box is quite low compared to the variance between the boxes indicating a clear underlying signal. This low spatial variance is consistent with the results obtained with the coarser resolution gridded data.

Given the significant frequencies, these contingency results could be used to make probability forecasts for the cold, average and warm terces given a forecast category selected using 1951-1995 data.

Predictability for July (figure 10) is much weaker than for August or July+August with significant correlations restricted to temperature over the UK and France. Only over the UK do the July temperature correlations compare well with the August figures.

The contingency table (table 2b) for the 4 French stations shows much reduced predictability for July compared to August. According to a chi square test, the correct forecasts are only significant at the 90% level. The reduced skill is most noticeable for the warm terce forecasts. Unlike the August forecasts, the frequency of warm observations following warm forecasts is not significantly greater than chance for the 4 stations nor for the 30 continental European stations where there is significant correlation between predictions and observed. Only the cold terce forecasts show skill in predicting cold terces and not predicting warm terces. Over the UK however, warm

observations do follow warm forecasts significantly more often than expected though warm observations were also found to be the most likely terce to follow average terce forecasts.

5. PREDICTABILITY FROM LOWER ORDER SST EIGENVECTORS

The previous sections show that there is considerable predictability of summer conditions over west-central Europe, based on EOF1 of North Atlantic SSTA. C97 found that SSTA EOF2, EOF3 and EOF4 did not significantly contribute to predictability of CET. However, the higher EOFs do contribute predictive skill for some of the predictands discussed in the previous two sections. The usefulness of other EOFs as predictors was examined by stepwise regression (Afifi and Azen, 1979) using an F test as the stepping criterion.

Stepwise regression experiments were carried out using July-August EWR and CET as predictands and time series for the first 8 EOFs of January-February north Atlantic SSTA as predictors. As in C97, the higher order EOFs do not add to CET prediction skill. However the time series of EOF2 (T2 in fig. 2b) does add to EWR prediction skill. Jack-knife regression predictions of July-August EWR were made using T1 and T2 (time series of EOF1 and EOF2) as predictors. The predicted and observed values for 1946-95 are shown in fig. 11. The correlation is 0.4, which is a substantial improvement on the skill using T1 alone (r=.31). Other EOFs produced no significant additional skill.

T2 is more dominated by low frequency variability than T1 and has a clear trend over the period 1946-95 (fig. 2). There also is a notable step in the series around 1970. This low frequency contribution is cause to be cautious about results. An example of a rainfall anomaly which corresponds better with the T2 series than the T1 series is the drought year of 1976 which is the year with the lowest T2 value. T1 does not show much signal in 1976.

Jack-knife predictions of western European mean temperature, SLP and rainfall were carried out using T2 instead of T1. Temperature predictability is very poor with insignificant correlations over most of western Europe. However, an extensive area of significant negative correlation for SLP stretches from the Baltic to the UK (fig. 12a). The significant correlations are located further north than those obtained with T1 (fig. 3c). Correlation scores for rainfall predictions with T2 (fig. 12b) are significant in a large area surrounding the North Sea, but the correlations are not very high anywhere, i.e. r always < 0.4.

6. SST and SLP COMPOSITES

Statistically significant relationships between winter North Atlantic SSTA and subsequent summer temperatures, pressure and rainfall have been described above. Statistics alone do not provide an explanation for the apparent long-lead predictability however. A mechanism linking winter SSTA with summer anomalies might be revealed by looking at typical behaviour in the intermediate months. For this purpose, years between 1946 and 1995 were subdivided into 5 categories. The categories were selected according to the observed and linear regression forecasts of July-August CET.

Category 1; Warm forecasts which were correct, ie. |Forecast-Observed| < 1C; forecast and observed CET both above average (16C).

Category 2; Warm forecasts which were too warm, ie. Observed-Forecast > 1C; forecast CET above average.

Category 3; Cold forecasts which were correct, ie. |Forecast-Observed| < 1C; forecast and observed CET both below average.

Category 4; Cold forecasts which were too cold, ie. Forecast-Observed > 1C; forecast CET below average.

Category 5; Remaining forecasts.

The number of years in categories 1 to 4 were 10,9,18 and 7 respectively. The least well fitting years were excluded from categories 1,2 and 3 to produce equal sized categories of 8 years. A year that just failed to qualify for category 4 (1969) was added to category 4 to give it the same number of cases as the other categories. The result is 4 distinct clusters of years as shown in fig. 13.

For each of the categories, average SSTA was calculated for January-February, March, April, May, June, and July-August. This provides an estimate of the progression of typical significant anomalies from the time of the forecasts (January-February) to the forecast period (July-August). The significances of the anomalies are calculated using a T test to determine if the anomalies are significantly different from the mean of the 10 surrounding years (the previous 5 years and subsequent 4 years). The use of relatively short 10 year averages was made to minimize the effect of trend in the results.

The anomalies for the correct warm forecasts (category 1) are shown in fig. 14. The January-February SSTA show a pattern very much like EOF 1 in fig. 1. In following months the warm west Atlantic SSTA near the USA shifts eastward (at a rate of about 15 degrees of longitude per month), reaching the east Atlantic off Europe by July-August. This movement is close to (south of) the track of the Gulf Stream extension across the Atlantic. The anomaly also follows the prevailing wind direction. The cool SSTA south of Greenland in Jan-Feb gradually weakens, but significant anomalies are still in that region in July-August. The warm SSTA around the UK and in the Baltic region gradually weakens, but revives in July-August, merging with the SSTA moving from the west Atlantic. By July-August, significant warm SSTA cover most of the west European continental shelf and stretch well out into the Atlantic.

The incorrect warm forecast years (category 2) have a Jan-Feb SSTA anomaly pattern similar to (but somewhat weaker than) that for the correct warm forecast years (fig. 15). Although positive SSTA in the North Sea/Baltic region persist until June, positive SSTA in the central/west Atlantic fade. By July-August 90% of the Atlantic SST north of 20N is colder than average, with significant anomalies in the east Atlantic near Europe.

The correct cool forecast (category 3) SSTA composite is similar to that for category 1 in Jan-Feb, but with opposite sign (fig. 16). Adjacent to the American coast the cold anomalies extend further north than do the warm anomalies in the warm forecast years. Although there is some north-eastward movement of these cold anomalies in following months, there is no evidence of the systematic movement to the east Atlantic that appeared for category 1. Instead, below average SSTA persists near Europe (and warm SSTA persists near Greenland) from Jan-Feb through to Jul-Aug.

The incorrect cool forecast (category 4) SSTA composite is similar to the correct cool forecast composite near Europe and America, but the warm anomalies to the near and to the south of Greenland are weaker

and less extensive (fig. 17). In following months cool SSTA develops in the central North Atlantic and warm SSTA develops near Europe.

Composites of SLP anomalies were also compiled for the above categories. Because there is less trend in SLP, SLP anomalies are calculated from the period average, 1948-1995. The Jan-Feb composite for category 1 (fig. 18) shows a clear and significant bipolar pattern, with low SLP anomalies north of 55N and high SLP anomalies to the south. Geostrophically this pattern gives westerly wind anomalies at UK latitudes. The pattern also shows a strong North Atlantic Oscillation (NAO) signal (Lamb and Peppler, 1987) with a stronger than average Azores high and a deeper than average Icelandic low. During March to June this pattern disappears, and composite SLP anomalies are insignificant. The pattern reappears in July-August with a low over Greenland and high over north-west Europe. The Jul-Aug SLP anomaly pattern is consistent with that predicted by positive Jan-Feb T1 (cf fig. 3). The reason for the loss of significance in intermediate months is not known.

For incorrect warm forecasts (fig. 19), the SLP composite also has a strong NAO-like bipolar signal in January-February, with the anomaly centres about 15 degrees further west than for the correct warm forecast composite. Again, the pattern disappears in March to June with very few SLP anomalies significant at the 5% level. In July-August a significant low SLP anomaly appears over north-west Europe.

The correct cool summer composite SLP pattern for January-February is almost the reverse of the correct warm summer equivalent. As with the warm summer composites, the patterns become weak and insignificant in the intermediate months (fig. 20). In July-August , there is a large area of significant positive anomalies in the north Atlantic north of 60N with weak anomalies to the south in the mid-latitudes including NW Europe. There is a weak northerly flow over the UK which is associated with cool summers. The incorrect cool summer SLP composite for January-February is similar to the correct cool composite pattern, but the anomaly centres are less extensive longitudinally (fig. 21) . Again the patterns weaken during the intermediate spring months. The July-August pattern shows high SLP anomaly over Scandinavia stretching SW towards the mid Atlantic but no NAO dipole. The cool forecast composites show high pressure to be pre-dominant in the Atlantic to the west of the UK during April to June prior to the correct forecast summers and vice versa prior to the incorrect forecast years, though the anomalies are weak and should be regarded with caution.

In summary, the composites show strong SSTA and SLP signals in January-February. The SSTA patterns slowly evolve during the intermediate months with a high degree of persistence in the East Atlantic, into anomaly patterns consistent with warm or cold NW Europe summers in July-August. The composite SLP anomaly patterns generally weaken in intermediate months but strengthen again in July -August. This suggests that the predictability signal is carried by the SSTA pattern rather than by some atmospheric signal.

8. DISCUSSION

The statistical results in sections 3-6 above show significant relationships between July-August temperature, rainfall and SLP in west-central Europe and preceding Jan-Feb North Atlantic SSTA. The results were obtained by straightforward regression methods, using datasets that have been carefully quality controlled. The relationships are physically consistent: high (low) temperatures over a wide area tend to occur when SSTA is warm (cool) near Europe and pressure is high (low) over Europe

The SSTA composites described in section 7 for particular categories indicate consistent SSTA evolution from Jan-Feb to Jul-Aug, with significant anomalies in intervening months: however no corresponding significant SLP evolution was detected. Rowell (1998) also found the atmosphere to behave independently of ocean temperature forcing by an analysis of variance of SLP in GCM ensemble simulations forced with observed SST. In his simulations, Rowell found that north Atlantic (40-60N) SLP variance explained by SST is at a clear annual minimum in March-May.

The composite SSTA averages for successful warm forecast years (category 1, fig. 14) suggest that anomalously warm SST moves across the Atlantic in a region south of the Gulf Stream track prior to warm NW European summers. Possible causes of the movement could be advection by ocean currents or transfer of heat by the atmosphere. Although the direction is consistent with prevailing ocean currents, advection can be discounted as a mechanism for the central-eastern Atlantic as ocean currents are not fast enough. Ocean currents of about 40cm/sec or 1000km/month would be needed to move the warm water at the speed shown in fig. 14. Shipdrift data (Richardson 1985) show that such speeds are only found near the eastern USA coast: further east, typical current speeds are nearer 10cm/sec.

Another explanation could be that the air above the warm (say) SST anomaly is heated by the warm SST, and advected to heat the sea surface water downwind. The positions of the warm anomalies in figure 14 are consistent with heat being transported by the prevailing west south-west wind across the Atlantic. To seek evidence that the atmosphere plays a role, for correct warm forecasts (category 1) composites of Night Marine Air Temperature Anomalies (NMATA) were calculated. The NMAT anomalies are very similar to SSTA (fig. 22). The NMATA warm pool crossing the Atlantic contains larger anomalies than the SSTA counterpart, with peak NMATA of 0.6C compared with peak SSTA of 0.4C. There is some evidence of the warm NMAT anomalies extending further NE ahead of the SSTA counterparts which is most noticeable in April. If heat is transferred by wind rather than ocean current then the air temperature would be expected to rise a little in advance of sea temperature. Also notable is that the cold NMATA to the south east of Greenland is less extensive than the SSTA equivalent.

The persistence of SSTA near Europe for successful forecasts suggests that the predictability might be simply due to the east Atlantic. The relative importance of eastern and western Atlantic SSTA was investigated by splitting EOF1 into two components, representing the Atlantic west of and east of 20W respectively, and calculating east and west projections T1E and T1W. (The projection is made simply by summing the products of the EOF1 weight and the SSTA for all the gridboxes in the relevant domain). The western Atlantic was found to be a better predictor of July-August CET than the eastern Atlantic: correlations of predicted and observed for 1946 to 1995 were 0.49 using T1W, and 0.42 using T1E compared with 0.51 for T1.

There is evidence of decadal timescale variability in the North Atlantic. Deser and Blackmon (1993) , Grotzner et al. (1996) and Sutton and Allen (1997) have identified 12-14 year cycles in the movement of large scale Atlantic surface temperature anomalies. Mysak and Power (1992) discuss similar cycles in North Atlantic/Arctic ice data. Such decadal cycles may influence European land conditions. The squared coherence between January-February T1 and July-August CET (fig. 23) shows a peak at 7-8 years (Squared coherence is a correlation like measure of how similarly 2 time series behave at a given frequency, (Bloomfield, 1976)) . Variability on this timescale is not so widely documented. However Moron et al.,(1998) and Mann and Park (1994) have detected SSTA variability on this timescale and

Rogers (1984) detected variability of winter NAO on this timescale. However this 7-8 year cycle is not strong enough to allow significant predictability at interannual or longer timescales. The maximum correlation between T1 and July-August CET at leads greater than 1 year is 0.1 (for a 7 year lead) which is well below the 5% significance level.

9. CONCLUSIONS

Using linear regression methods, an empirical relationship between western European summer conditions and preceding winter SSTA has been identified. Using the Jan-Feb projection of EOF1 of SSTA as a predictor, forecasts of Jul-Aug conditions were made over several decades. Correlations of predicted and observed values suggest that predictions with limited but potentially useful skill can be made at a 4 month lead time for temperature, rainfall and surface pressure over wide areas of NW Europe. The level of skill compares well with that found in other studies (eg. Johansson et al., 1998).

Temperature is the most predictable of these three variables: correlation between independent forecasts of mean temperature and observed values for 1951-1995 exceeds 0.5 over NE France, the Low Countries and SE England. Significant skill (5% level) extends over British Isles, Germany, most of France, northern Spain, the Alpine Countries, Western Poland and Southern Sweden and also over parts of estern Canada and NE USA. SLP and rainfall skill is less high when measured by correlation than the temperature skill. Time coefficients of the first two north Atlantic SSTA eigenvectors (T1 and T2) predict rainfall and SLP over a similar region to the temperature predictions, The predictors are best used separately: T1 for the Low Countries and for Germany and Alpine countries south of 50 N; and T2 for the UK, NE Germany and Southern Scandinavia. The regions with 5% significant predictability are shown in fig. 12.

Temperature prediction skill over the UK is concentrated in the second half of July and August and is highest for SE England and East Anglia. Predictions of temperature for regions further south east such as eastern France are better in August than July. Predictions for periods of 1 month or less for the UK are generally less accurate than predictions for 45 or 60 day averages. Possible explanations for the predictability include persistence of cold or warm temperature anomalies in the NW Europe vicinity throughout spring. This theory was found to fit cold years better than warm years. In warm years there is evidence of anomalously warm SSTA crossing the Atlantic during the spring months. A possible explanation for this movement is heat transfer downwind by surface winds.

Dynamical seasonal forecasting systems are also under development at UKMO and elsewhere. Information from empirical and dynamical systems is already used jointly for some tropical region forecasts (Ward et al, 1993). In the future, it is expected that empirical predictions such as those described in this paper will be combined with dynamical predictions to maximise skill.

ACKNOWLEDGEMENTS

Thanks to Tracy Basnett, Briony Horton, David Cullum from the Hadley Centre and Mark New, Mike Hulme and Phil Jones from Climate Research Unit, Norwich for providing data for this work.

REFERENCES

Afifi, A.A., and Azen, S.P. 1979. 'Statistical Analysis, a computer orientated approach.' 2nd ed. Acad.Press.

Barnston, A.G. 1994. 'Linear statistical short-term climate predictive skill in the northern hemisphere.' *J.Climate*, **7**, 1513-1564.

Barnston, A.G. and Smith, T.M. 1996. 'Specification and prediction of global surface temperature and precipitation from global SST using CCA.' *J.Climate*, **9**, 2660-2697.

Basnett, T. and Parker, D.E. 1997. 'Development of the global mean sea level pressure data set GMSLP2.' *UK Met. Office Climate Res. Tech. Note* **79**.

Bloomfield, P. 1976. 'Fourier analysis of time series. An Introduction.' *Wiley & Sons*, New York.

Carson, D.J. 1998. 'Seasonal *Forecasting' Q.J.R.Meteorol.Soc.*, **124**, 1-26.

Colman, A.W. 1997. 'Prediction of summer central England temperature from preceding north Atlantic winter sea surface temperature.' *Int. J. Climatol.*, **17**, 1285-1300.

Colman, A.W. and Davey, M.K. 1996. 'Linear regression forecast of central England temperature for July-August 1996.' *Long Lead Bull.*, **5** no.2 Published by NOAA/NWS, USA.

Colman, A.W. and Davey, M.K. 1997. 'Linear regression forecast of central England temperature for July-August 1997.' *Long Lead Bull.*, **6** no.2 Published by NOAA/NWS, USA.

Deser, C. and Blackmon, M.L. 1993. 'Surface climate variations over the north Atlantic ocean during winter: 1900-1989.' *J.Climate*, **6**, 1743-1753.

Folland, C.K., Owen, J., Ward, M.N. and Colman, A.W. 1991. 'Prediction of seasonal rainfall in the Sahel region using empirical and dynamical methods.' *J.Forecast.*, **10**, 21-56.

Gregory, J.M., Jones, P.D. and Wigley, T. 1992. 'Precipitation in Britain: an analysis of area averaged data updated to 1989.' *Int.J.Climatol.*, **11**, 331.

Grotzner, A., Latif, M., and Barnett, T.P. 1996. 'A decadal climate cycle in the north Atlantic ocean as simulated by the ECHO coupled GCM.' Max Planck Institut fur Meteorologie Report 208.

Harrison, M.S.J. 1995. 'Long range forecasting since 1980: empirical and numerial prediction out to 1 month for the United Kingdom.' *Weather*, **50**, 440-448.

Hastenrath, S. 1995. 'Recent advances in tropical climate prediction.' *J.Climate*, **8**, 1519-1532.

Hulme, M. 1994. 'Validation of large scale precipitation fields in general circulation models.' *Global precipitation and climate change*, NATO ASI **I26**, 387-405.

Johansson, A., Barnston, A., Saha, S. and Van den Dool, H. 1998. 'On the level and origin of seasonal forecast skill in Europe.' *J.Atmos.Sci.*, **55**, 103-127.

Jones, P. D. 1994. 'Hemispheric surface air temperature variations, a reanalysis and an update to 1993.' *J.Climate*, **7**, 1794-1802.

Lamb, P.J. and Pepler, R.A. 1987. 'North Atlantic Oscillation; concepts and an application.' *Bull.Am.Meteorol.Soc.*, **68**, 1218-1225.

Manley, G. 1974. 'Central England temperatures, monthly means 1659 to 1993.' *Q.J.R.Meteorol.Soc.*, **79**, 242-261.

Mann, M.E. and Park, J. 1994. 'Global-scale modes of surface temperature variability on interannual to century timescales.' *Geophys.res.let.*, **99**, 25819-25833.

Moron, V., Vautard, R. and Ghil, M. 1998. 'Trends, interdecadal and interannual oscillations in global sea-surface temperatures.' *Climate Dynamics* **14**, 545-569.

Mysak, L.A. and Power, B.S. 1992. 'Sea Ice anomalies in the western Arctic and Greenland-Iceland sea and their relation to an interdecadal climate cycle.' *Climatol.Bull.*, **26**, 147-176.

Palmer, T.N. and Anderson, D.L.T. 1995. 'The prospects for seasonal forecasting - a review paper.' *Q.J.R.Meteorol.Soc.*, **120**, 755-793.

Parker, D.E., Legg, T. & Folland, C.K. 1992. 'A new daily central England temperature series, 1772-1991.' *Int.J.Climatol.*, **12**, 317-342.

Parker, D.E., Folland, C.K. and Jackson, M. 1995. 'Marine surface temperature: Observed variations and data requirements.' *Climate Change* **31**, 559-600.

Ratcliffe, R.A.S. and Murray, R. 1970. 'New lag associations between north Atlantic sea temperatures and European pressure applied to long range weather forecasting.' *Q.J.R.Meteorol.Soc.*, **96**, 226-246.

Rayner, N.A., Horton, E.B., Parker, D.E., Folland, C.K., and Hackett, R.B. 1996. 'Version 2.2 of the global sea ice and sea surface temperature dataset, 1903-1994.' *UK Met. Office Climate Res. Tech. Note* **74**.

Richardson, P.L. 1985. 'Average velocity and transport of the gulf stream near 55W.' *J.Marine.Res.*, **43**, no.1.

Rogers, J.C. 1984. 'The association between the North Atlantic Oscillation and the Southern Oscillation in the northern hemisphere.' *Mon.Wea.Rev.*, **112**, 1999-2015.

Ropelewski, C.F and Halpert, M.S. 1987. 'Global and regional scale precipitation patterns associated with El nino/Southern oscillation.' *Mon.Wea.Rev.*, **115**, 1606-1626.

Rowell, D.P. 1998. 'Assessing potential seasonal predictability with an ensemble of multi-decadal GCM simulations.' *J.Climate* , **11**, 109-120.

Sutton, R.T. and Allen, M.R. 1997. 'Decadal predictability in the north Atlantic.' *Nature*, **388**, no. 6642, 563-567.

Ward, M.N., Folland, C.K., Maskell, K., Colman, A.W., Rowell, D.P. and Lane, K.P. 1993. 'Experimental seasonal forecasting of tropical

rainfall at the UK Meteorological Office.' *Prediction of interannual climate variations*, NATO ASI **I6**, 197-216.

FIGURE CAPTIONS

Figure 1: Eigenvectors (EOFS) of January-February North Atlantic SSTA between 20 and 80 north from MOHSST6C data for 1901-90. EOF 1 (a) explains 25.0% of total variance and EOF 2 (b) explains 13.5%.

Figure 2: a) Jan-Feb T1 (solid line),July-August CET (dotted line) 1946-1995. b) Jan-Feb T2 1946-1995. Correlation between CET and T1=0.53, correlation between CET and T2=0.12.

Figure 3: Correlations between jack-knife predictions from Jan-Feb T1 and July-August observations of a) surface temperatures 1951-1994, b) SLP 1951-1994, c) Precipitation 1951-1994 and d) surface temperatures 1901-1950.

Figure 4: Contour plot of correlation skill of Jack-knife forecasts, using projections of EOF1 as predictor for running pairs of calendar months for all lead times from 0-11 months. The projections of EOF 1 were also calculated from 2 month SSTA. Shading indicates significant correlations.

Figure 5: Correlations between observed monthly mean CET and jack-knife predictions from north Atlantic SSTA EOF time series. Forecasts for July-August have 4-6 month lead and forecasts for other months 2-6 month lead. The predictors are selected using stepwise regression.

Figure 6: Correlations between Jack-knife predictions and observed July 16 - August 31 district temperatures, 1956-1995 using Jan-Feb T1 as predictor.

Figure 7: Correlations between jack-knife predictions (from Jan-Feb T1) and August observations of a) surface temperatures 1951-1994, b) SLP 1951-1994, c) Precipitation 1951-1994 and d) surface temperatures 1901-1950.

Figure 8: Mean August temperature for 4 stations in Eastern France (solid line) plotted against Jack-knife forecasts from Jan-Feb T1 (dashed line) 1951-1995. Correlation between forecasts and observations = 0.75.

Figure 9: Contingency assessment of predictions of August mean temperatures from Jan-Feb T1 for individual stations and 10 UK districts shown in fig. 5. The predictions and observations for 1951-1995 are both categorised into 15 year terces. The 9 maps show the frequencies of the 9 possible observed/predicted terce combinations for each station and UK district for 1951-1995. Bold numbers are significant according to a chi squared test.

Figure 10: Correlations between jack-knife predictions (from Jan-Feb T1) and August observations of a) surface temperatures 1951-1994, b) SLP 1951-1994, c) Precipitation 1951-1994 and d) surface temperatures 1901-1950.

Figure 11: Jack-knife forecasts (solid line) of July-August EWR from a 2 variable regression equation using T1 and T2 as predictors plotted against observed EWR (dashed line) 1946-1995. Correlation between forecasts and observations = 0.40

Figure 12: Correlations between jack-knife predictions from Jan-Feb T2 and July-August observations 1951-1994 for a) SLP and b) precipitation.

Figure 13: Scatterplot of forecast v observed July-August CET showing the 4 clusters of years (identified by 4 different symbols) used to calculate composite means.

Figure 14: Mean SSTA for category 1 years (correct warm forecasts) for (a) January-February, (b) March, (c) April, (d) May, (e) June and (f) July-August. Category 1 years are 1949, 1952, 1975, 1983, 1984, 1989, 1990 and 1991.

Figure 15: Same as fig. 14 but for category 2 years (incorrect warm forecasts). Category 2 years are 1950, 1954, 1972, 1973, 1974, 1988, 1992 and 1993.

Figure 16: Same as fig. 14 but for category 3 years (correct cold forecasts). Category 3 years are 1956, 1965, 1968, 1977, 1978, 1980, 1985 and 1986.

Figure 17: Same as fig. 14 but for category 4 years (incorrect cold forecasts). Category 4 years are are 1947, 1955, 1959, 1966, 1969, 1970, 1976 and 1979.

Figure 18: Mean SLP anomaly for category 1 years (correct warm forecasts) for (a) January-February, (b) March, (c) April, (d) May, (e) June and (f) July-August. SLP anomalies are with respect to 1961-1990 averages.

Figure 19: Same as fig. 18 but for category 2 years.

Figure 20: Same as fig. 18 but for category 3 years.

Figure 21: Same as fig. 18 but for category 4 years.

Figure 22: Same as fig. 14 but for NMAT.

Figure 23: Squared coherences between Jan-Feb T1 and July-August CET; 1946-1995 (solid line). Dotted lines how 95% confidence intervals.

TABLE 1 Correlations between predicted and observed CET, using the projection of the leading SSTA EOF as the predictor. The EOF is calculated for 1901-1990 using different regions and datasets (vertical columns), and the projection is calculated using different datasets (horizontal rows).

a) Jackknife predictions 1946-1995
b) Linear regression (dependent) 1871-1995

	GISST1		MOHSST6C		MOHSST6B		GISST22		MOHSST6B enhanced	
EOF	(A)	(B)	(A)	(B)	(A)	(B)	(A)	(B)		
GISST1 40N-70N	.47	.40	.46	.41	.49	.44	.43	.37	.47	.31
MOHSST6C 40N-70N	.49	.42	.47	.39	.51	.44	.41	.37	.46	.32
MOHSST6C 20N-80N	.47	.42	.49	.39	.52	.45	.43	.38	.48	.38

TABLE 2a

VERIFICATION OF TERCE PREDICTIONS FOR 4 STATIONS IN NORTHERN FRANCE (PARIS LE BOURGET, BOURGES,DIJON,NANCY) FOR AUGUSTS 1951-1995

		FORECAST TERCE		
		1	2	3
OBSERVED TERCE	1	39	9	12
	2	19	32	9
	3	2	19	39

TABLE 2b

VERIFICATION OF TERCE PREDICTIONS FOR 4 STATIONS IN NORTHERN FRANCE (PARIS LE BOURGET, BOURGES,DIJON,NANCY) FOR JULYS 1951-1995

		FORECAST TERCE		
		1	2	3
OBSERVED TERCE	1	30	18	12
	2	23	15	22
	3	7	27	26

Figure 1; 1901–90 Atlantic 20–80N MOHSST6C Eigenvectors

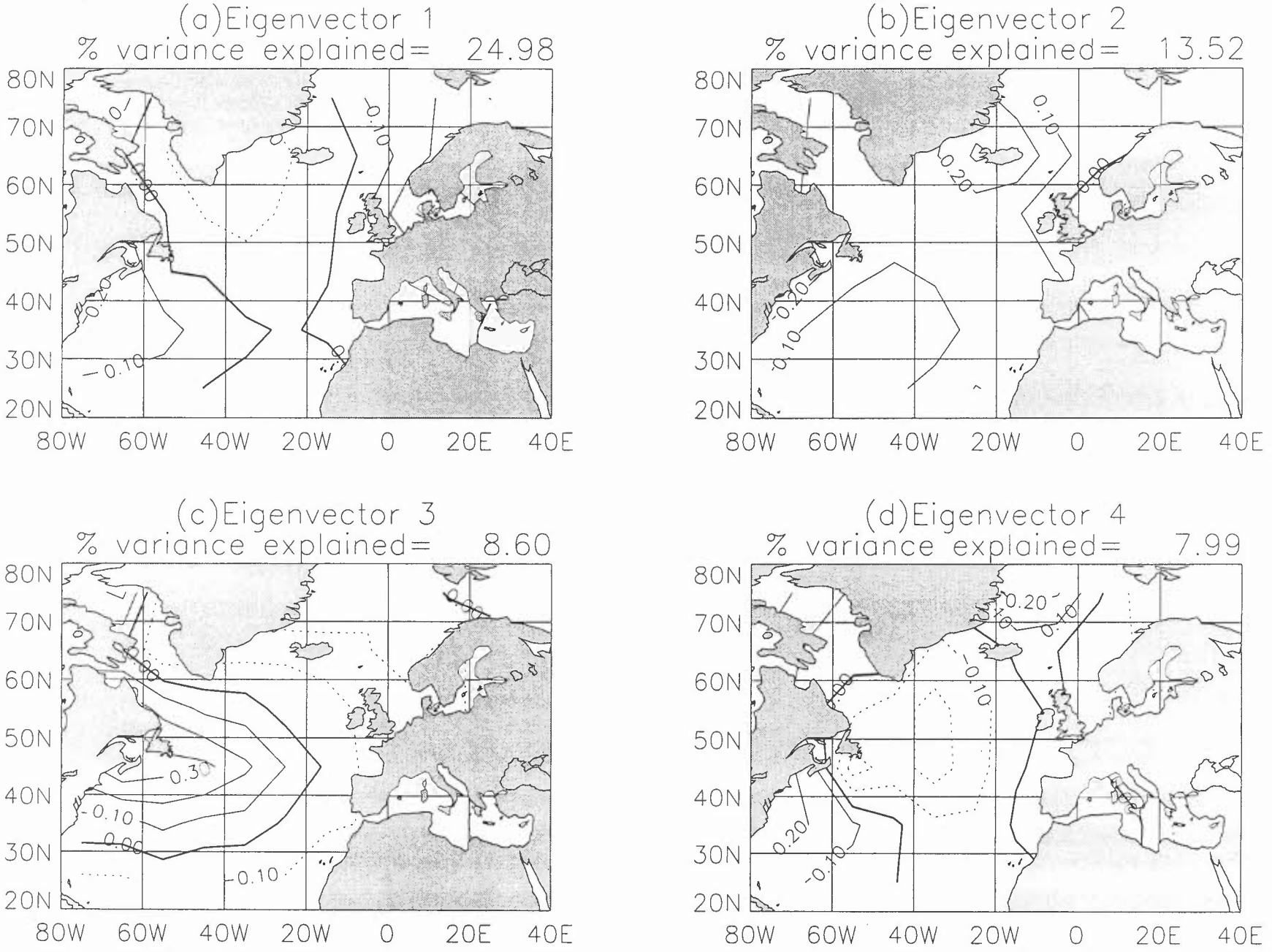

FIGURE 2a

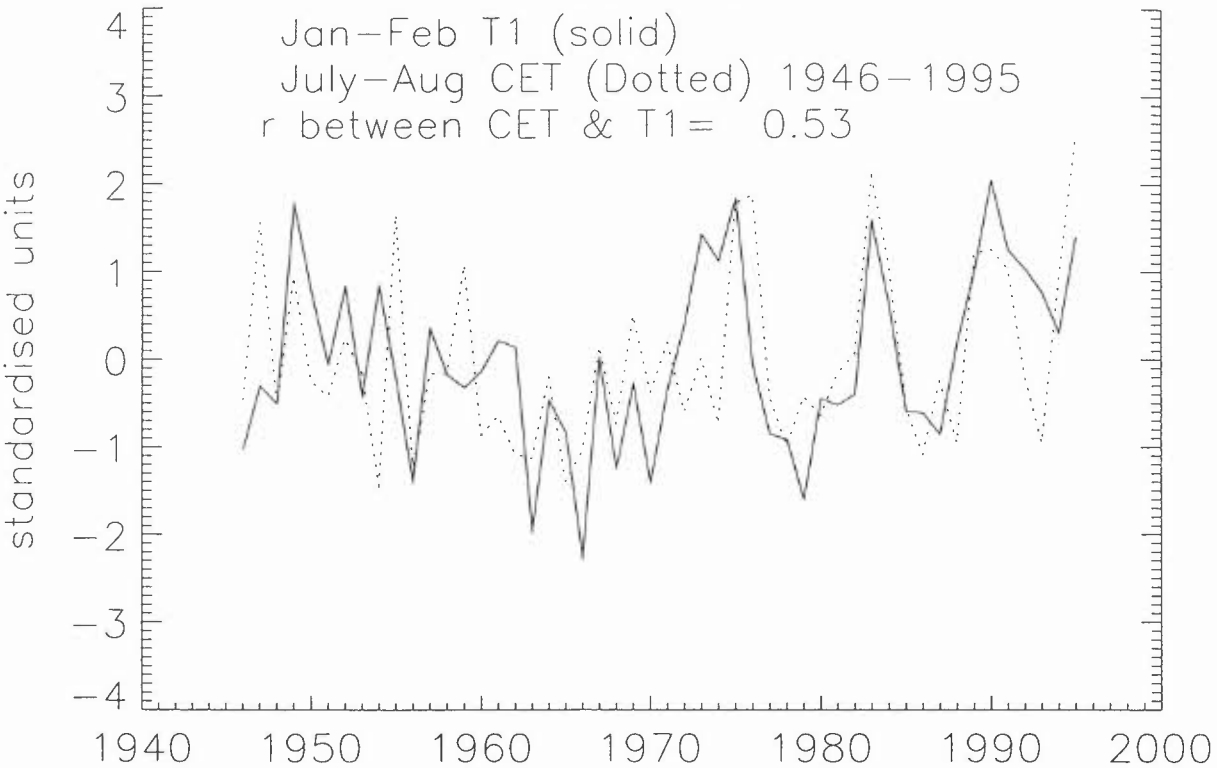

FIGURE 2b

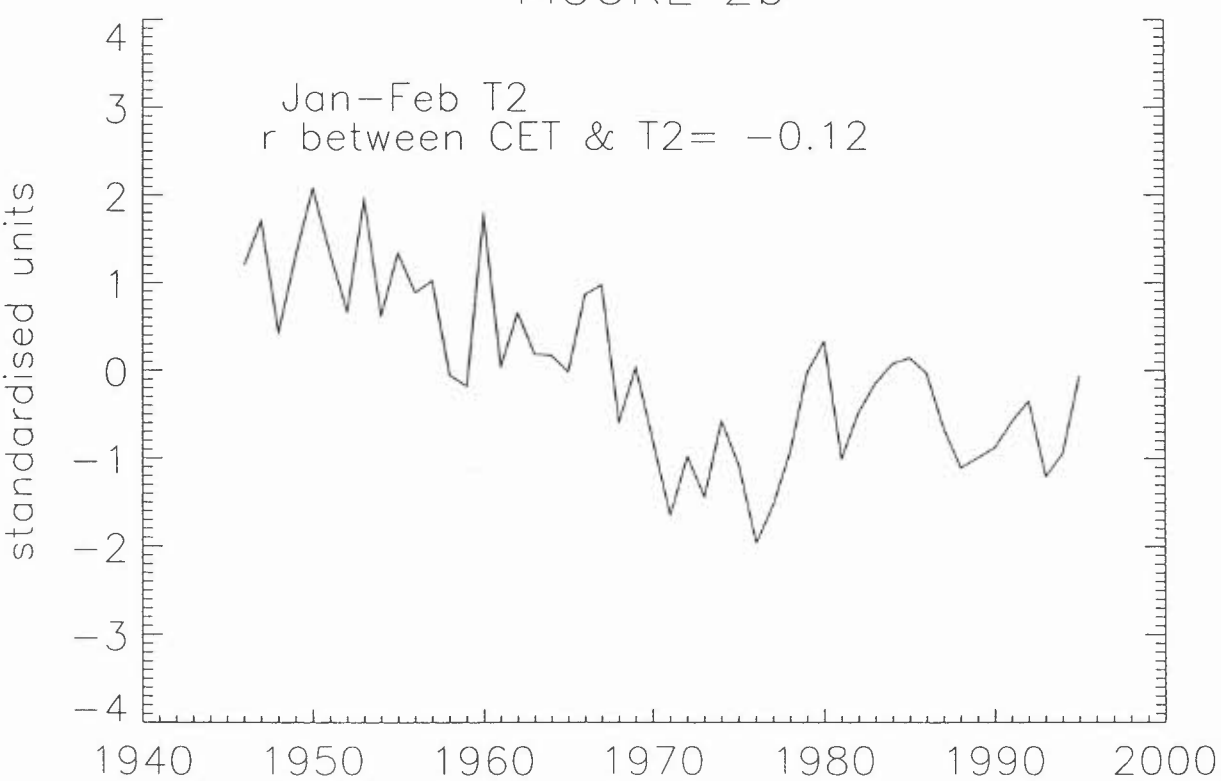

Figure 3

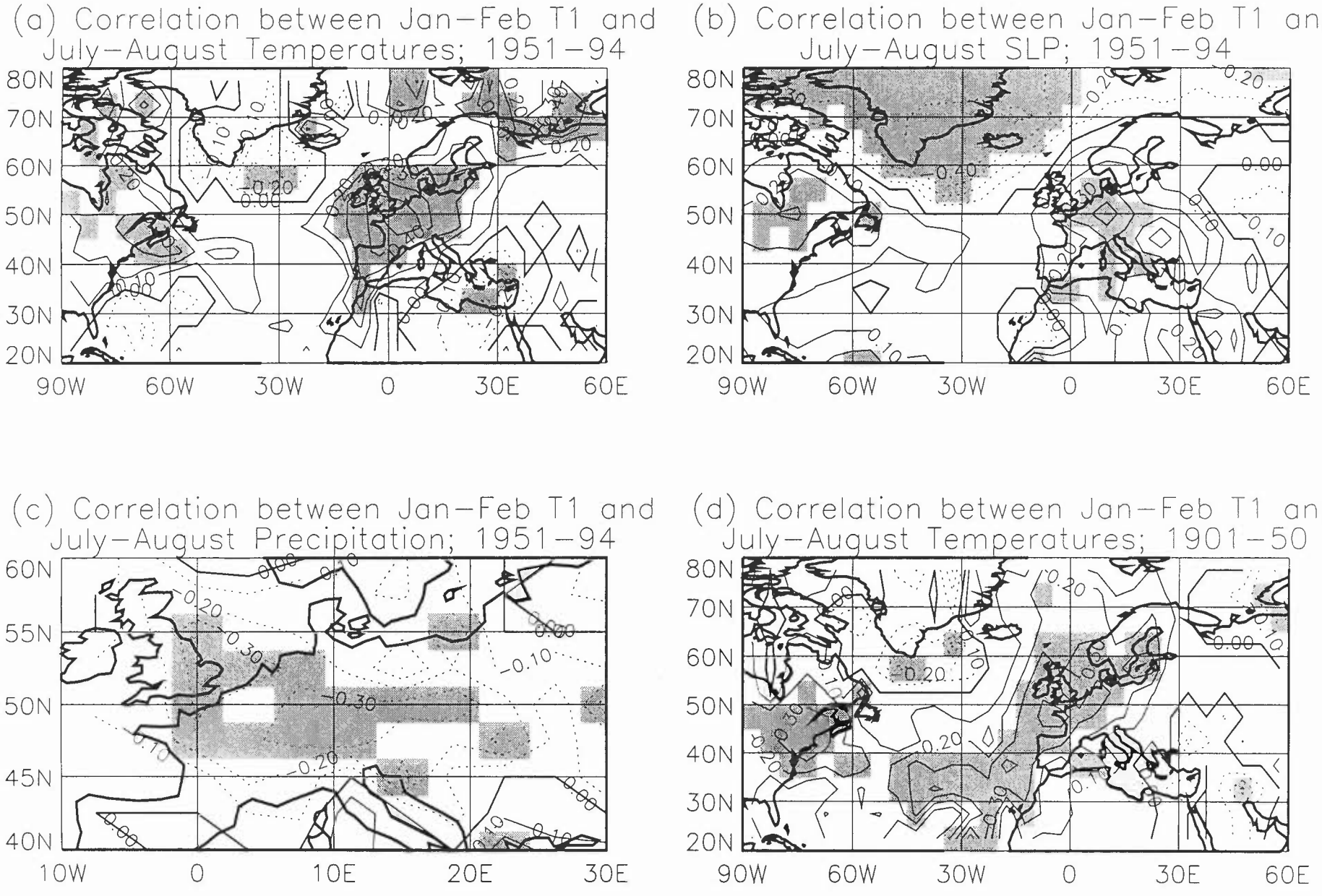
(a) Correlation between Jan–Feb T1 and July–August Temperatures; 1951–94
80N
70N
60N
50N
40N
30N
20N
90W
60W
30W
0
30E
60E
(b) Correlation between Jan–Feb T1 and July–August SLP; 1951–94
80N
70N
60N
50N
40N
30N
20N
90W
60W
30W
0
30E
60E
(c) Correlation between Jan–Feb T1 and July–August Precipitation; 1951–94
60N
55N
50N
45N
40N
10W
0
10E
20E
30E
(d) Correlation between Jan–Feb T1 and July–August Temperatures; 1901–50
80N
70N
60N
50N
40N
30N
20N
90W
60W
30W
0
30E
60E

Figure 4; contour plot of correlation skill,
significant correlations are hatched

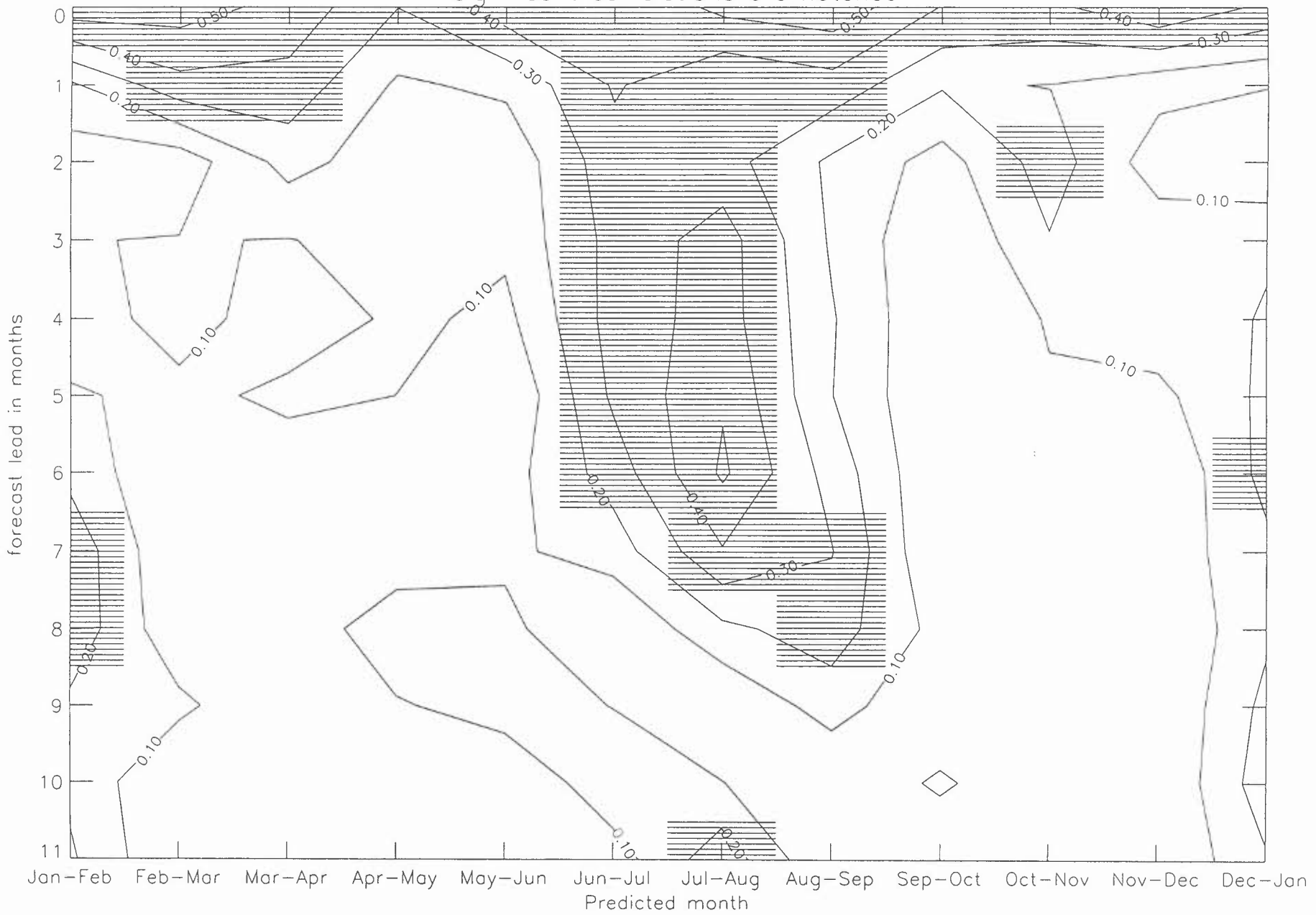

Figure 5: Jackknife Correlation between long lead predictions and observed CET 1946-95

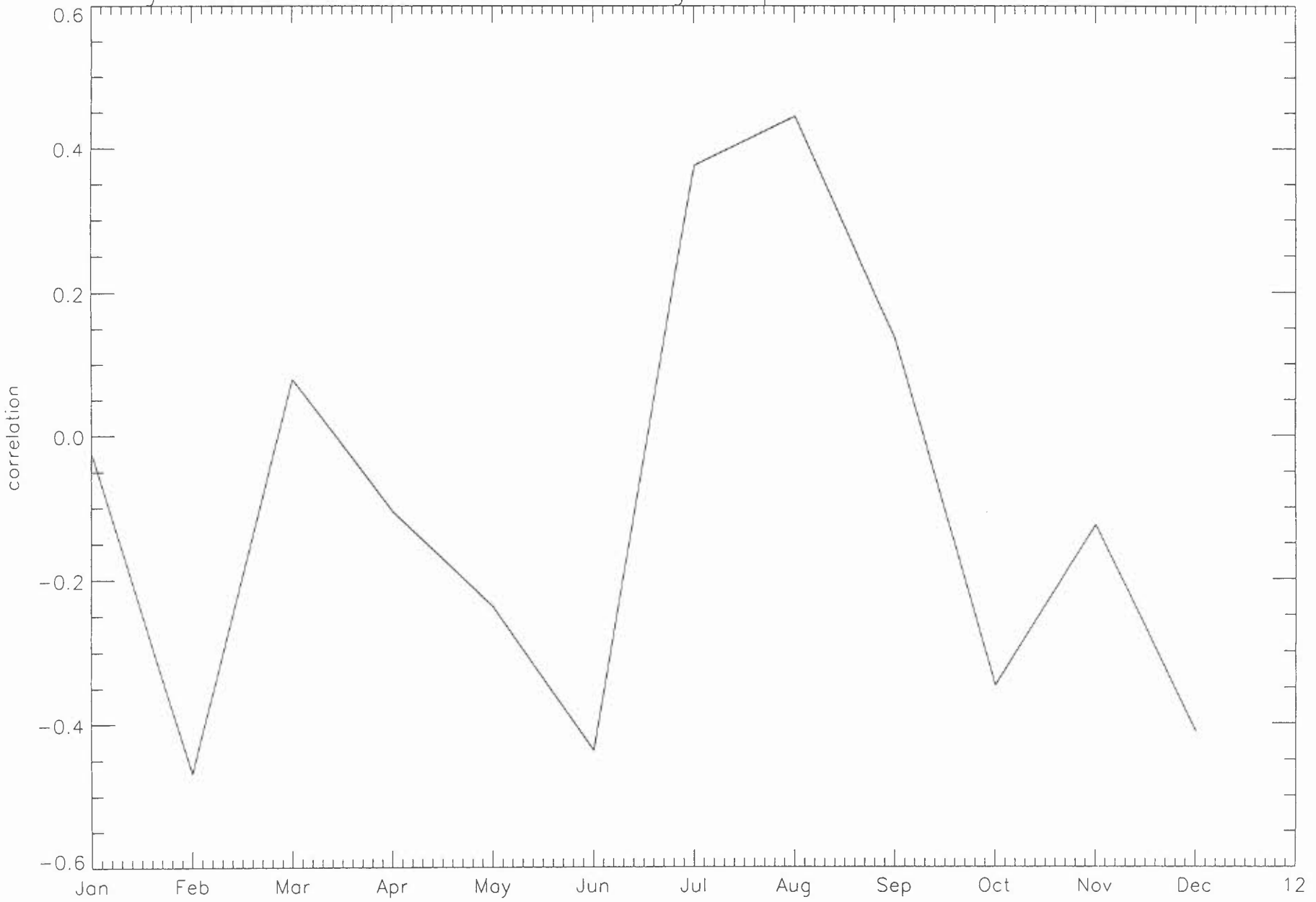

Figure 6: Correlation between Jack-knife predictions of district temperature and observed temperature 1956-95

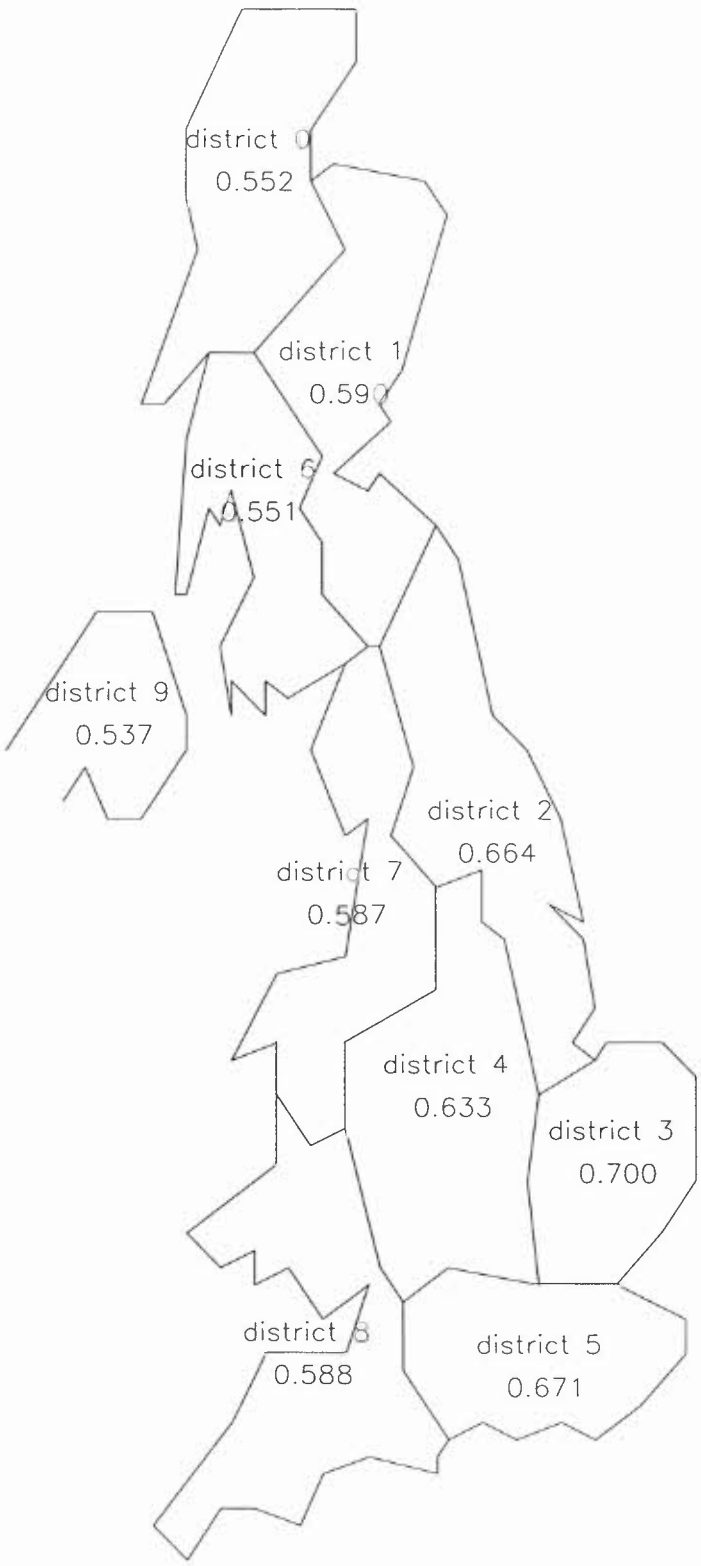

Figure 1

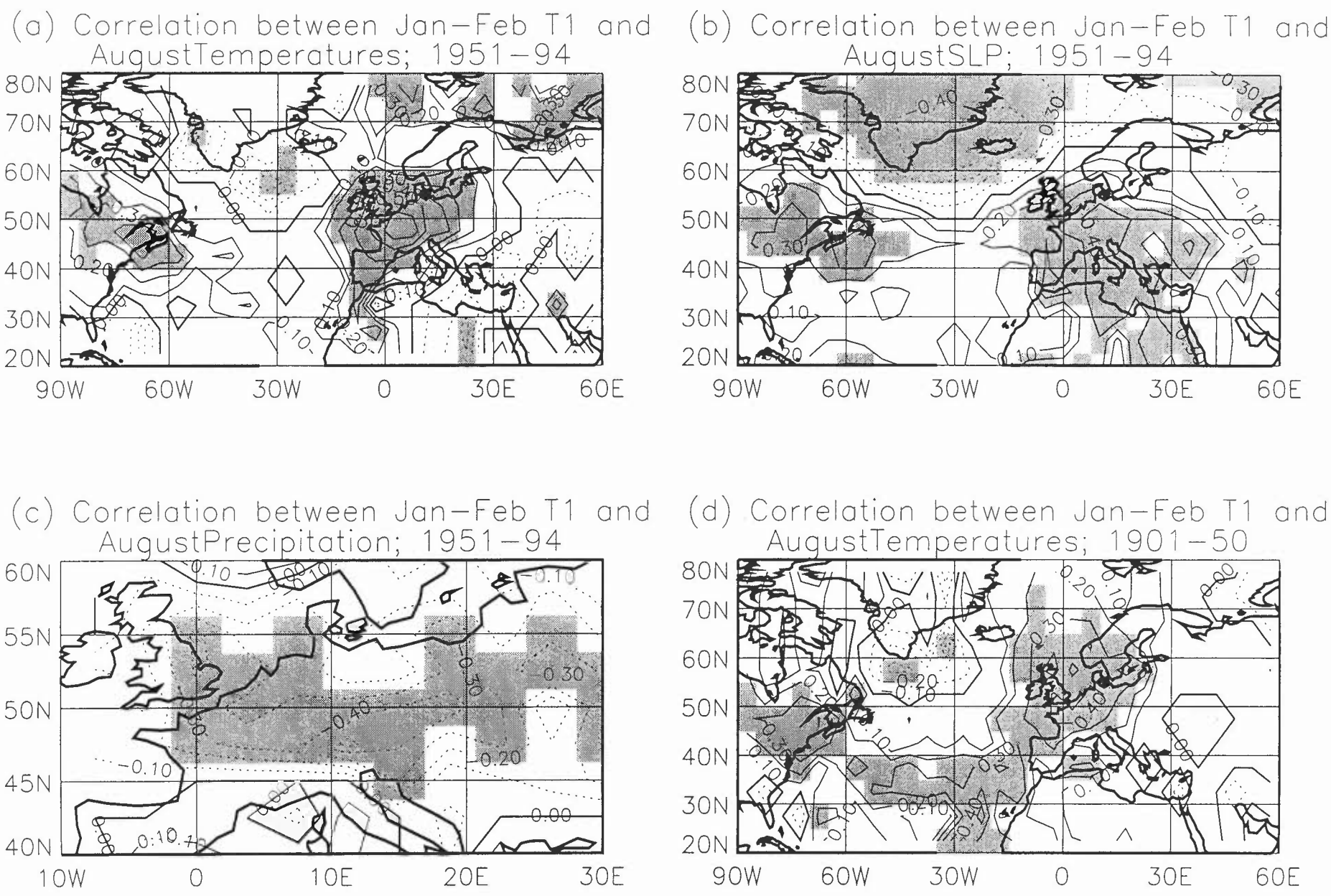
(a) Correlation between Jan–Feb T1 and AugustTemperatures; 1951–94
80N
70N
60N
50N
40N
30N
20N
90W
60W
30W
0
30E
60E
(b) Correlation between Jan–Feb T1 and AugustSLP; 1951–94
80N
70N
60N
50N
40N
30N
20N
90W
60W
30W
0
30E
60E
(c) Correlation between Jan–Feb T1 and AugustPrecipitation; 1951–94
60N
55N
50N
45N
40N
10W
0
10E
20E
30E
(d) Correlation between Jan–Feb T1 and AugustTemperatures; 1901–50
80N
70N
60N
50N
40N
30N
20N
90W
60W
30W
0
30E
60E

Figure 8:
Mean August temperature for Central East France (46.25–48.75N,1.875–6.5E) (Solid)
v Jackknife Forecast from JF ENA 20–80N EOF 1 GISST3 TS (dashed)

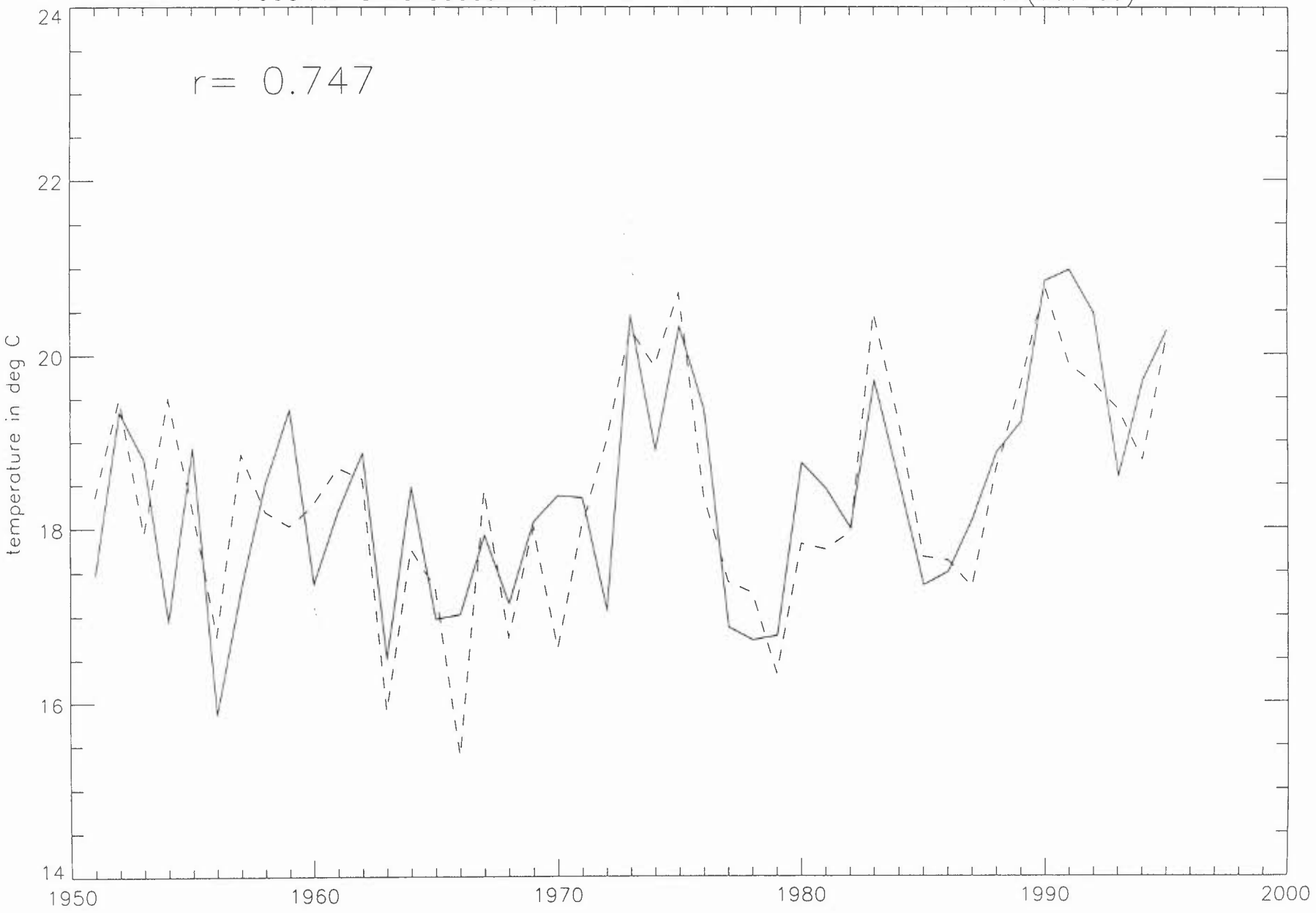

Figure 9

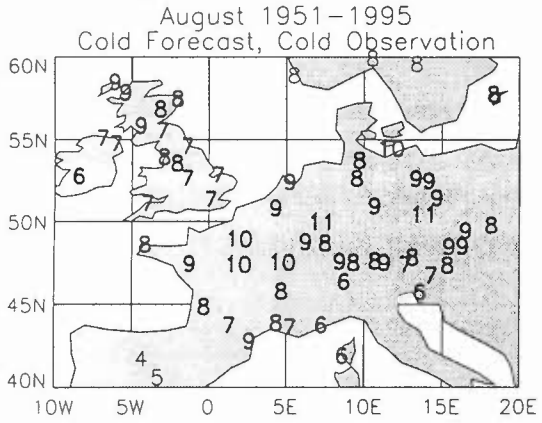
August 1951–1995
Cold Forecast, Cold Observation
60N
55N
50N
45N
40N
10W 5W 0 5E 10E 15E 20E

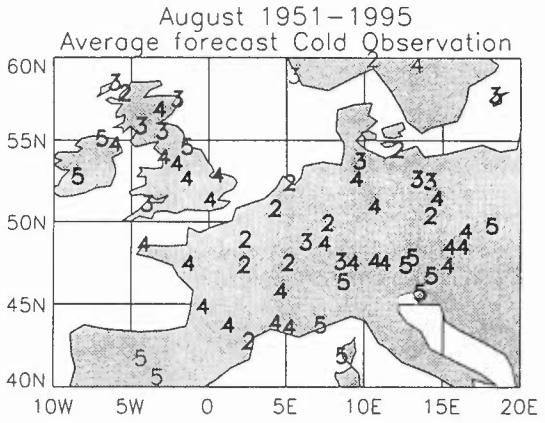
August 1951–1995
Average forecast Cold Observation
60N
55N
50N
45N
40N
10W 5W 0 5E 10E 15E 20E

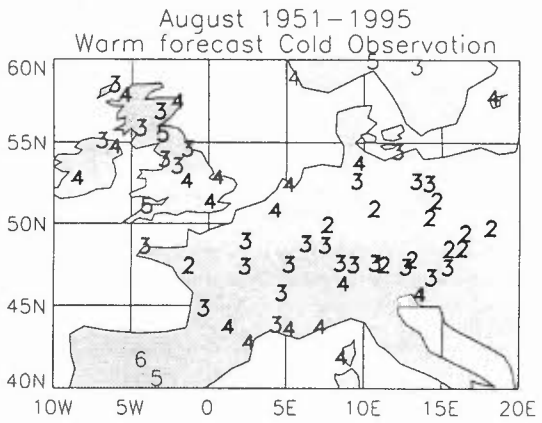
August 1951–1995
Warm forecast Cold Observation
60N
55N
50N
45N
40N
10W 5W 0 5E 10E 15E 20E

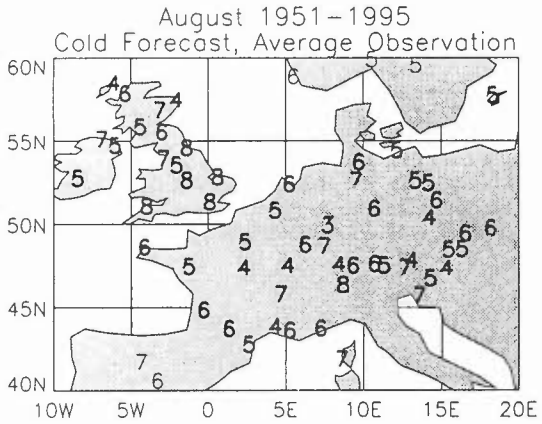
August 1951–1995
Cold Forecast, Average Observation
60N
55N
50N
45N
40N
10W 5W 0 5E 10E 15E 20E

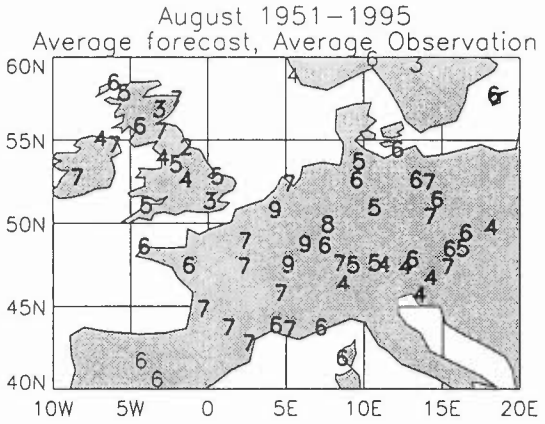
August 1951–1995
Average forecast, Average Observation
60N
55N
50N
45N
40N
10W 5W 0 5E 10E 15E 20E

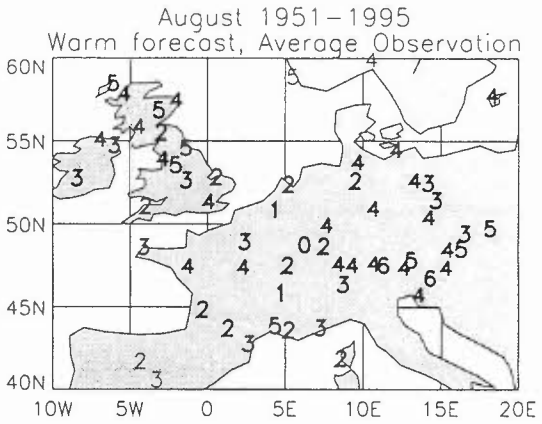
August 1951–1995
Warm forecast, Average Observation
60N
55N
50N
45N
40N
10W 5W 0 5E 10E 15E 20E

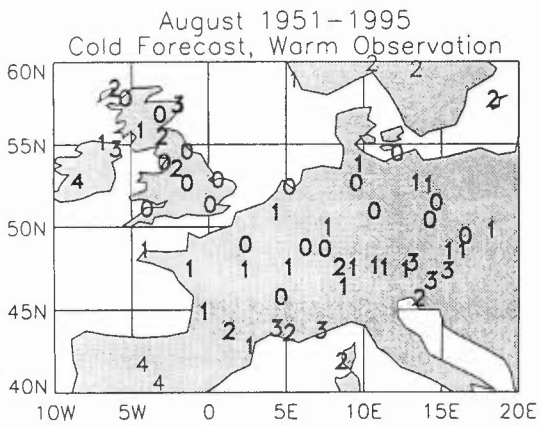
August 1951–1995
Cold Forecast, Warm Observation
60N
55N
50N
45N
40N
10W 5W 0 5E 10E 15E 20E

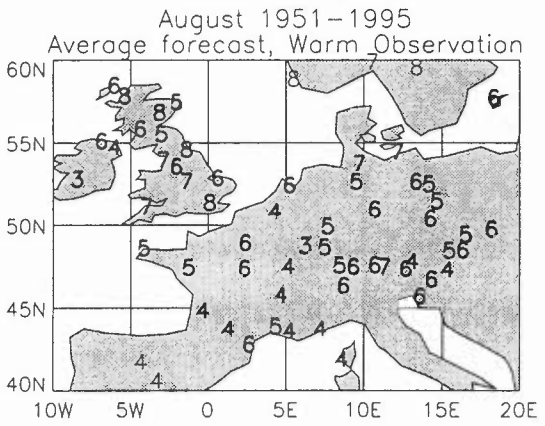
August 1951–1995
Average forecast, Warm Observation
60N
55N
50N
45N
40N
10W 5W 0 5E 10E 15E 20E

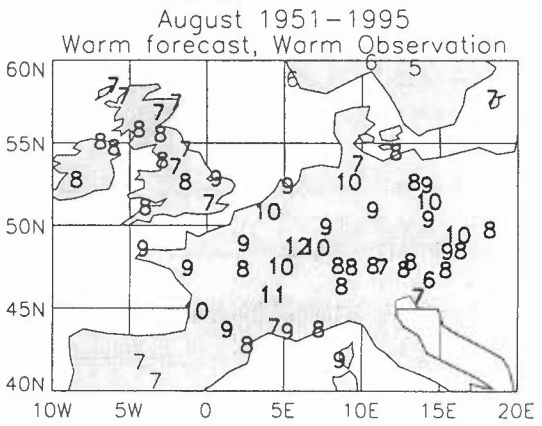
August 1951–1995
Warm forecast, Warm Observation
60N
55N
50N
45N
40N
10W 5W 0 5E 10E 15E 20E

Figure 10:

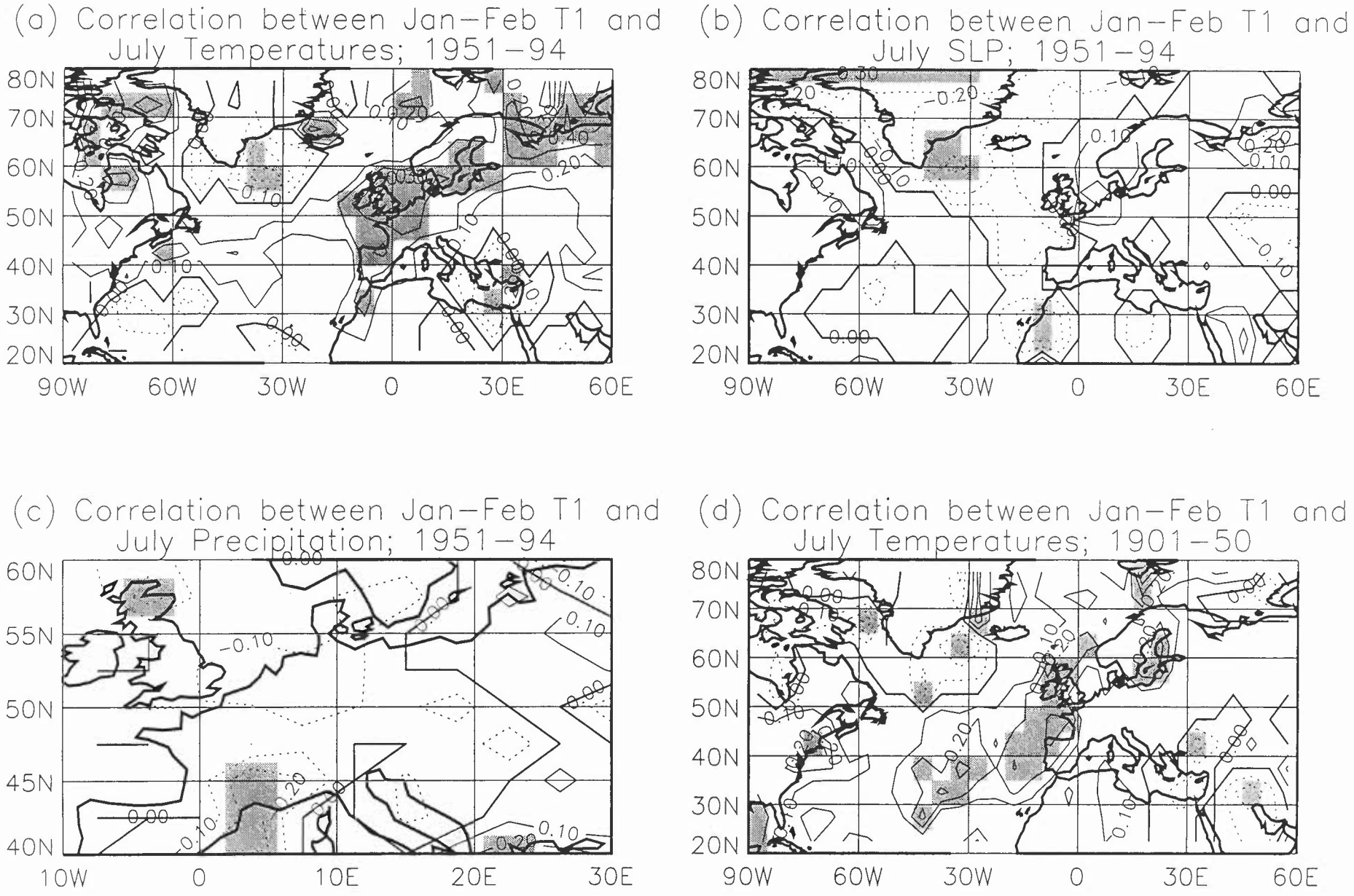
(a) Correlation between Jan–Feb T1 and July Temperatures; 1951–94
80N
70N
60N
50N
40N
30N
20N
90W
60W
30W
0
30E
60E
(b) Correlation between Jan–Feb T1 and July SLP; 1951–94
80N
70N
60N
50N
40N
30N
20N
90W
60W
30W
0
30E
60E
(c) Correlation between Jan–Feb T1 and July Precipitation; 1951–94
60N
55N
50N
45N
40N
10W
0
10E
20E
30E
(d) Correlation between Jan–Feb T1 and July Temperatures; 1901–50
80N
70N
60N
50N
40N
30N
20N
90W
60W
30W
0
30E
60E

Figure 11

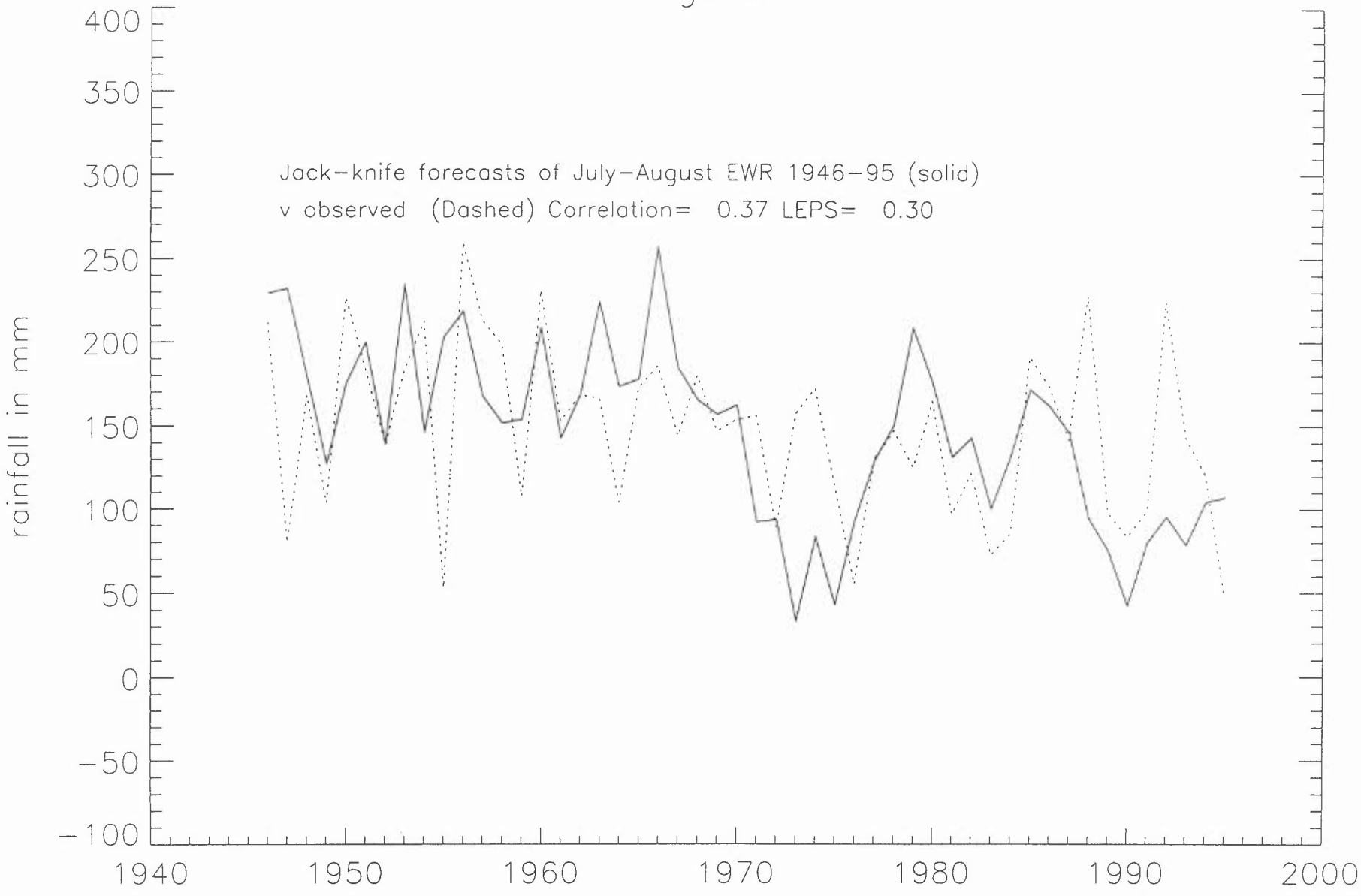
Jack-knife forecasts of July-August EWR 1946-95 (solid)
v observed (Dashed) Correlation= 0.37 LEPS= 0.30
rainfall in mm
400
350
300
250
200
150
100
50
0
-50
-100
1940
1950
1960
1970
1980
1990
2000

Figure 12a: Correlation between Jan–Feb T2 and July–August SLP; 1951–94

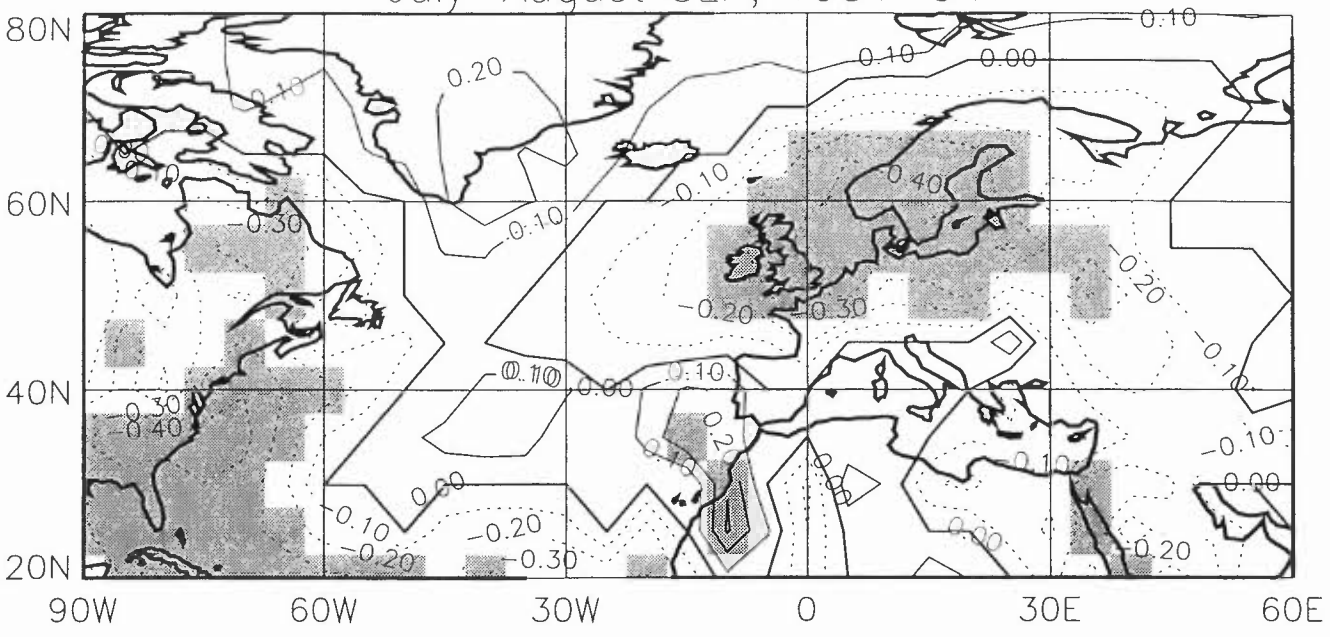

Figure 12b: Correlation between Jan–Feb T2 and July–August Precipitation; 1951–94

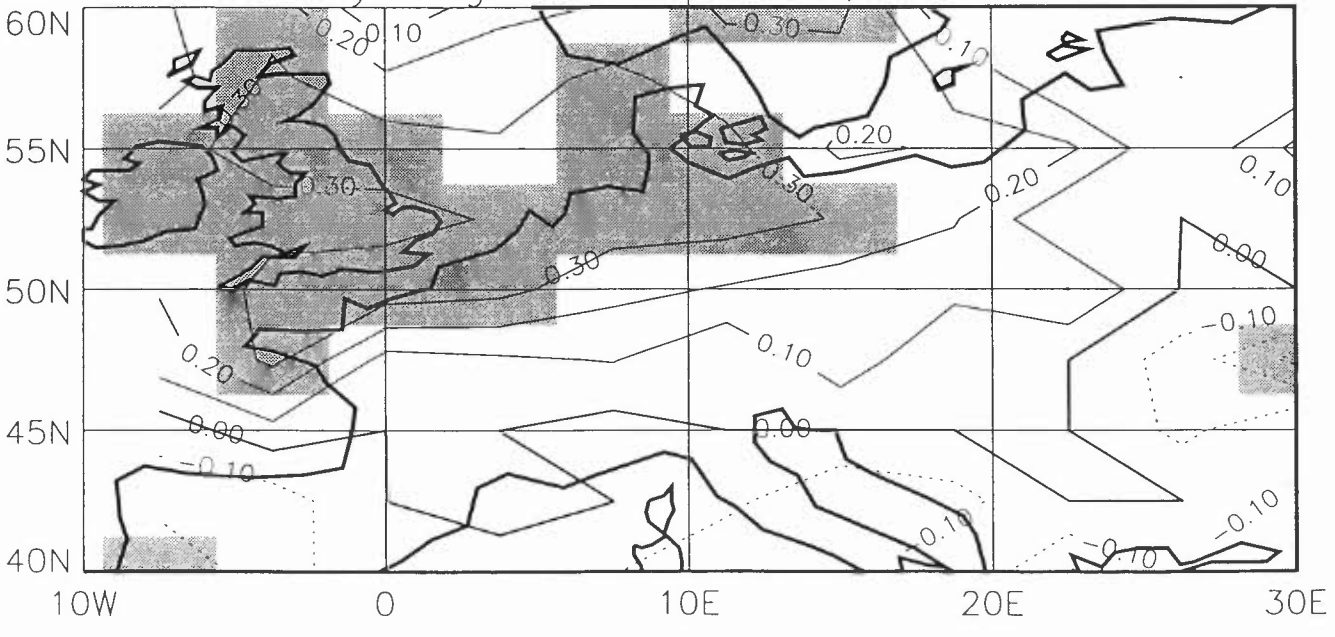

Figure 13

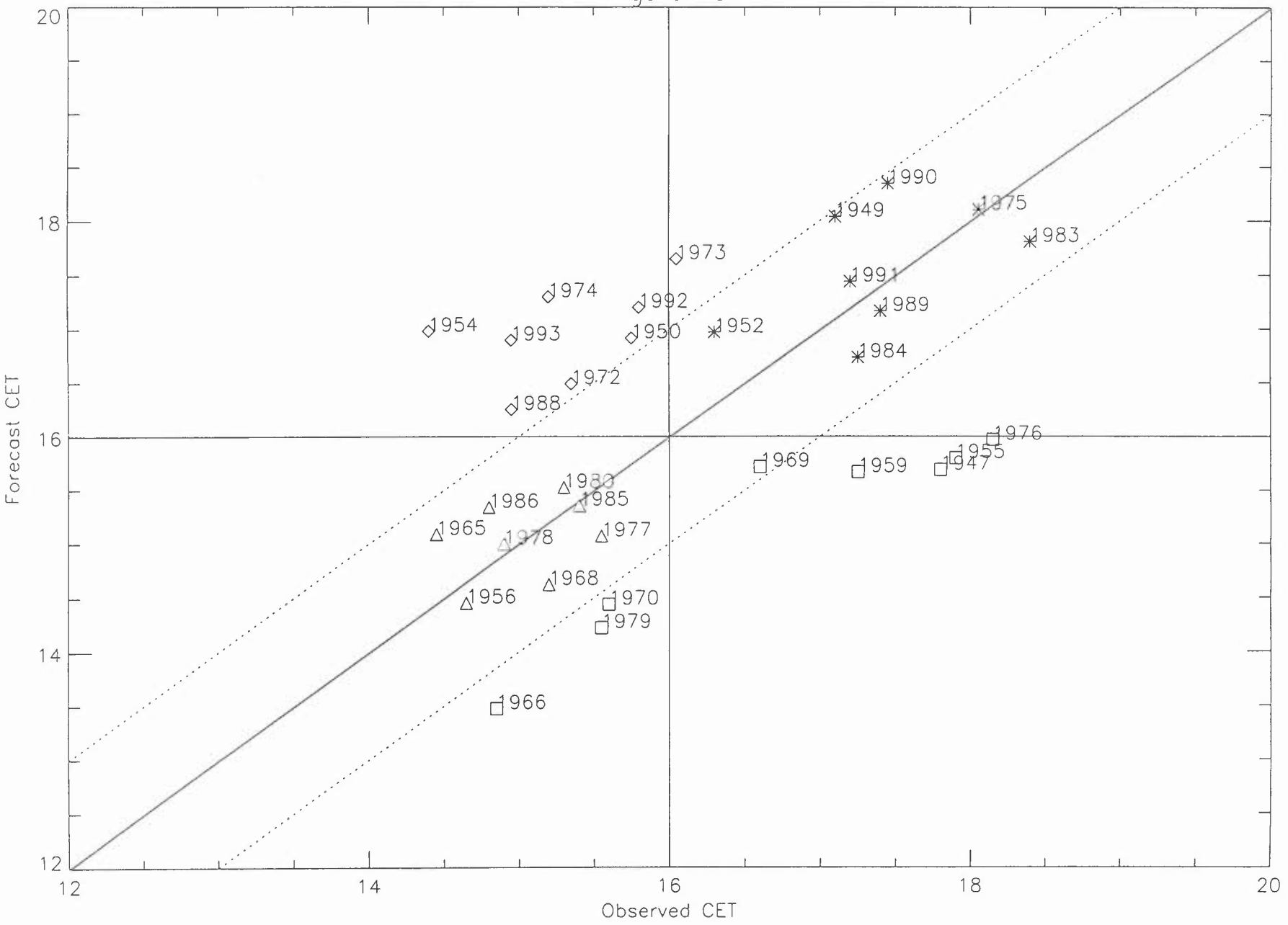
20
18
16
14
12
12
14
16
18
20
Forecast CET
Observed CET
1990
1949
1975
1983
1973
1991
1974
1992
1989
1954
1993
1950
1952
1984
1972
1988
1976
1955
1969
1959
1947
1980
1985
1986
1965
1978
1977
1968
1956
1970
1979
1966

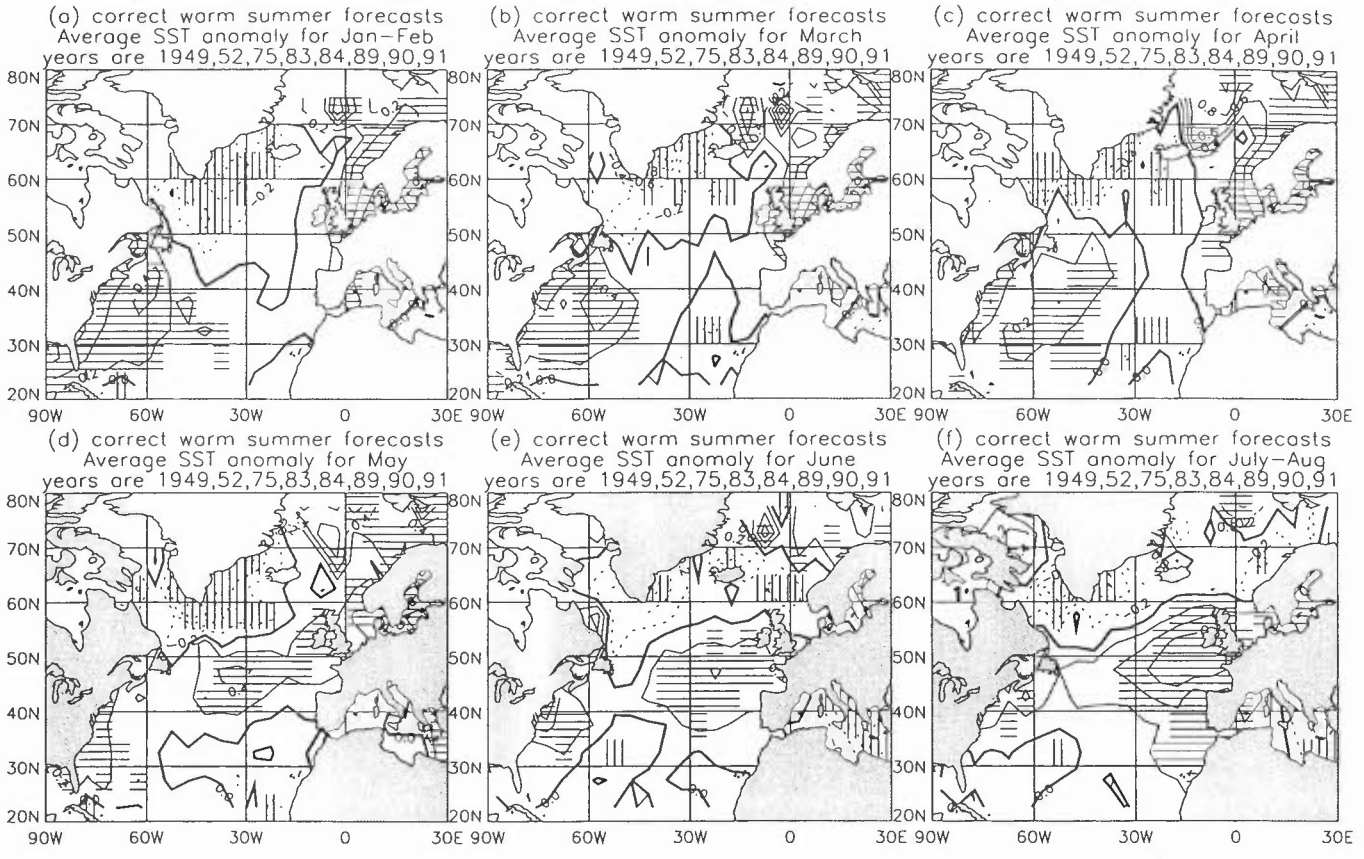

FIGURE 14

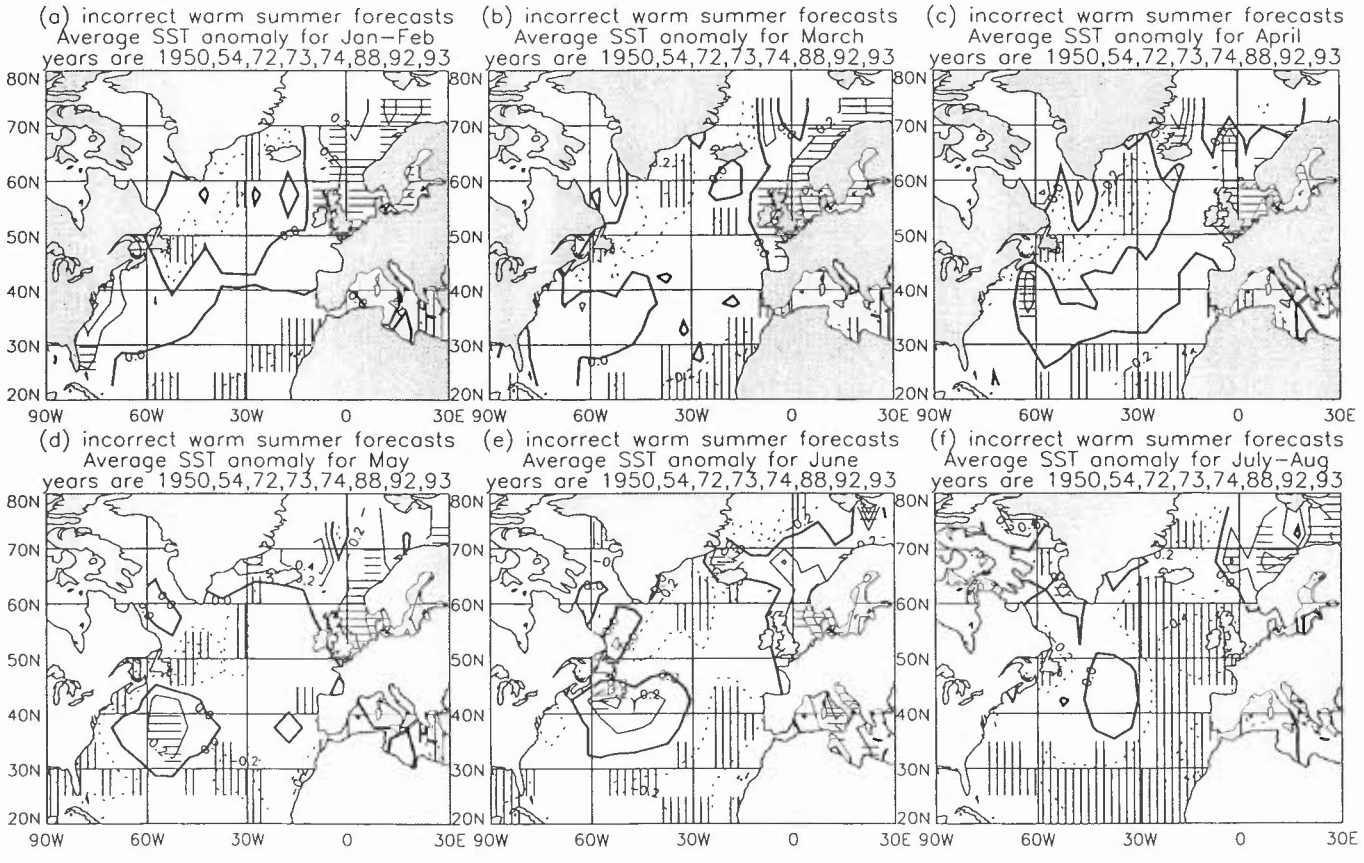

FIGURE 15

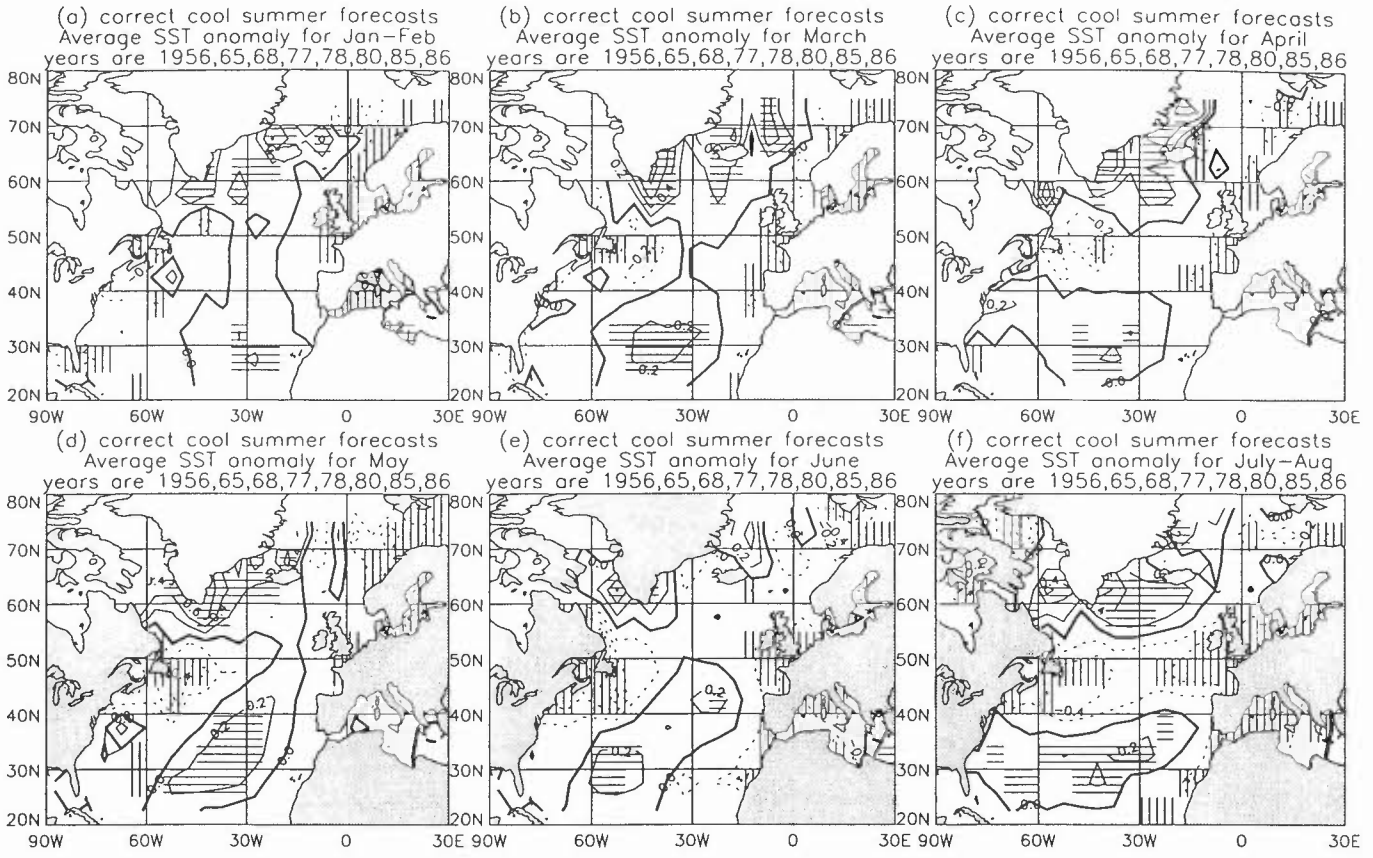

FIGURE16

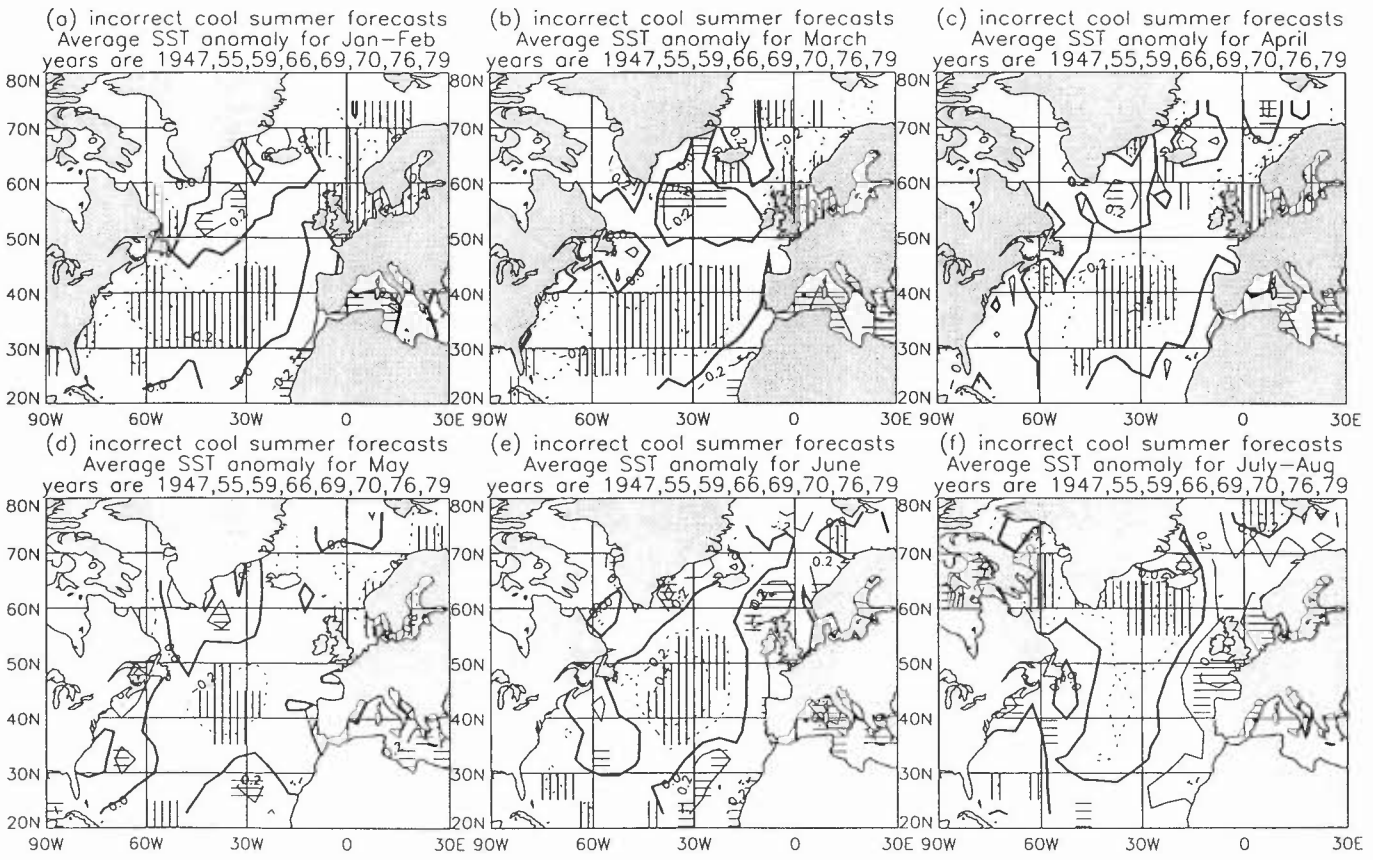

FIGURE17

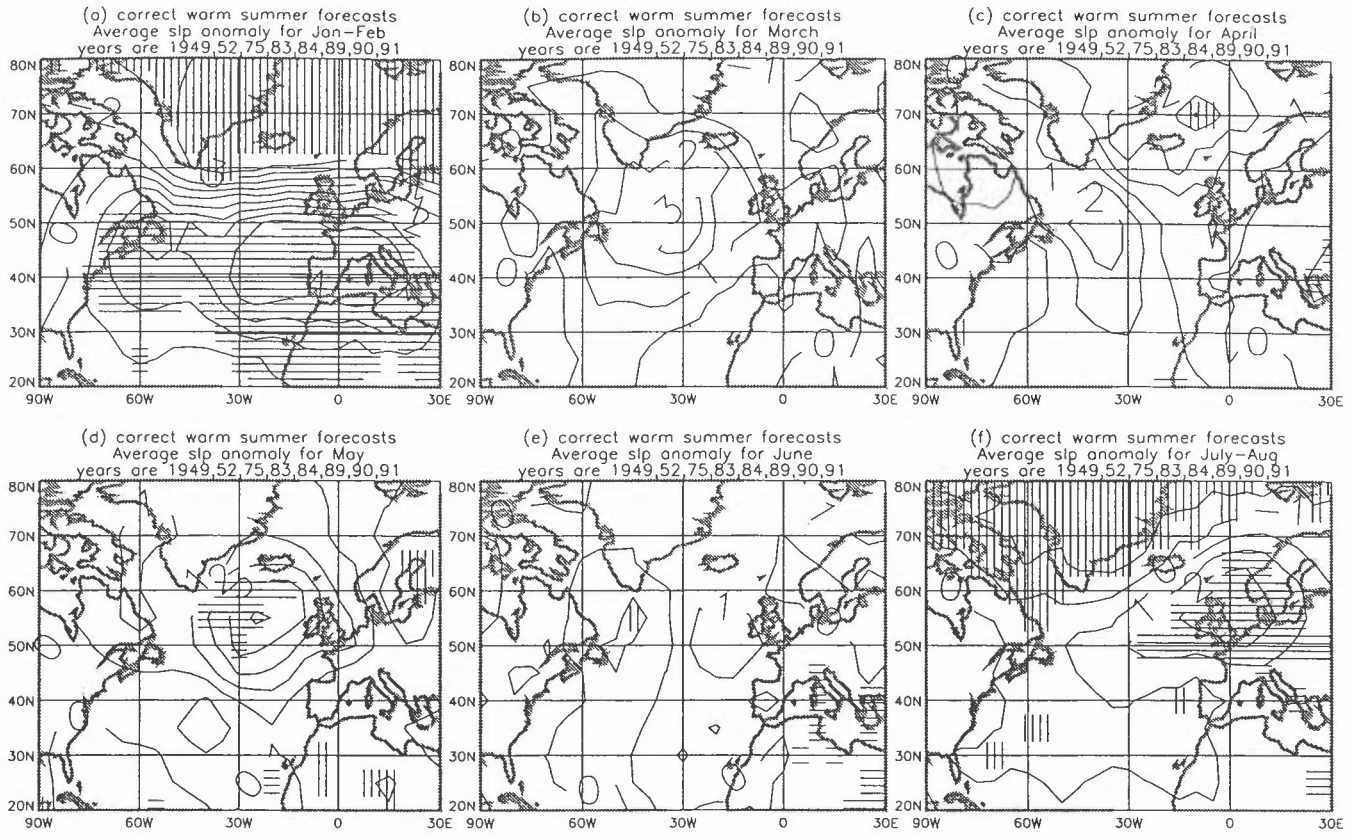

FIGURE 18

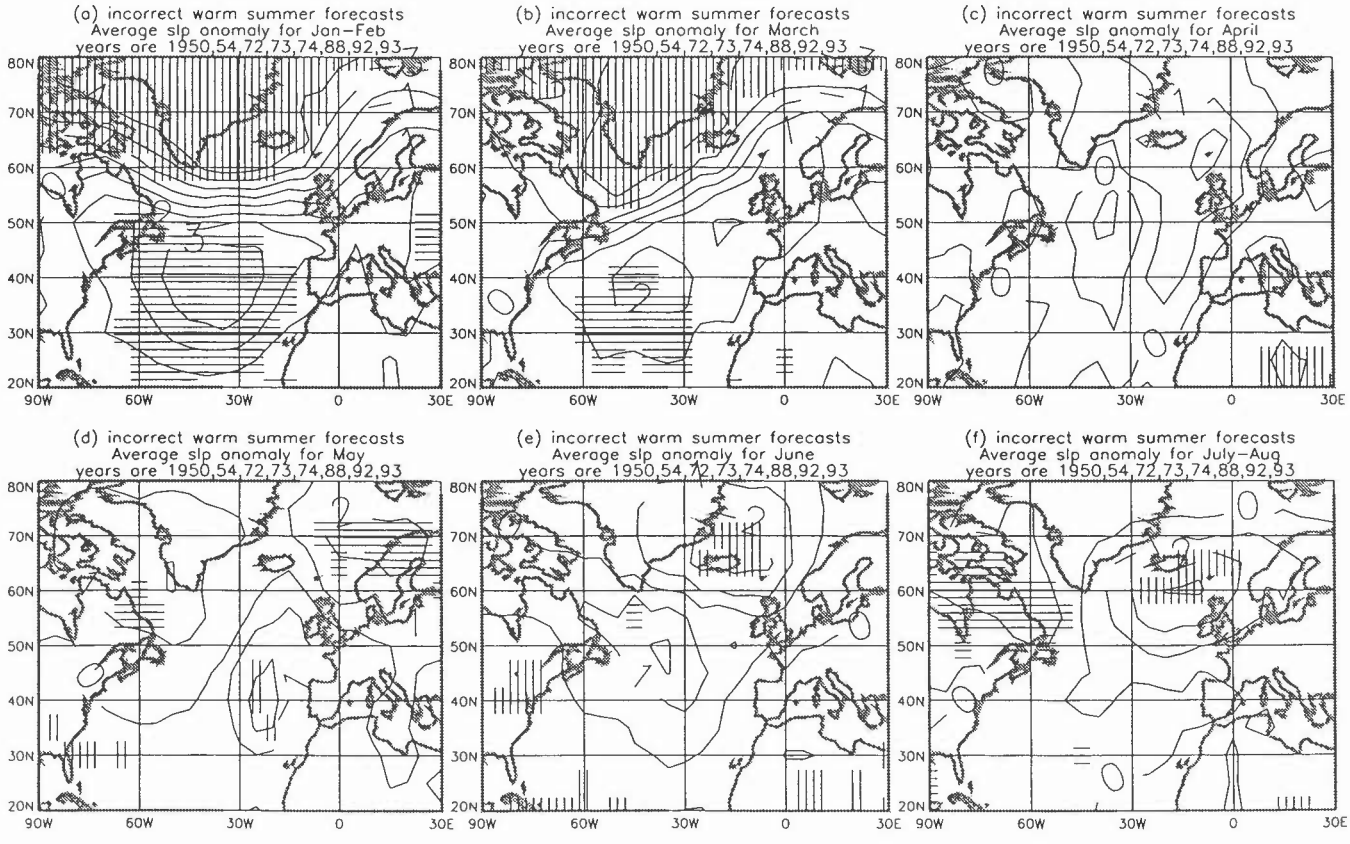

FIGURE 19

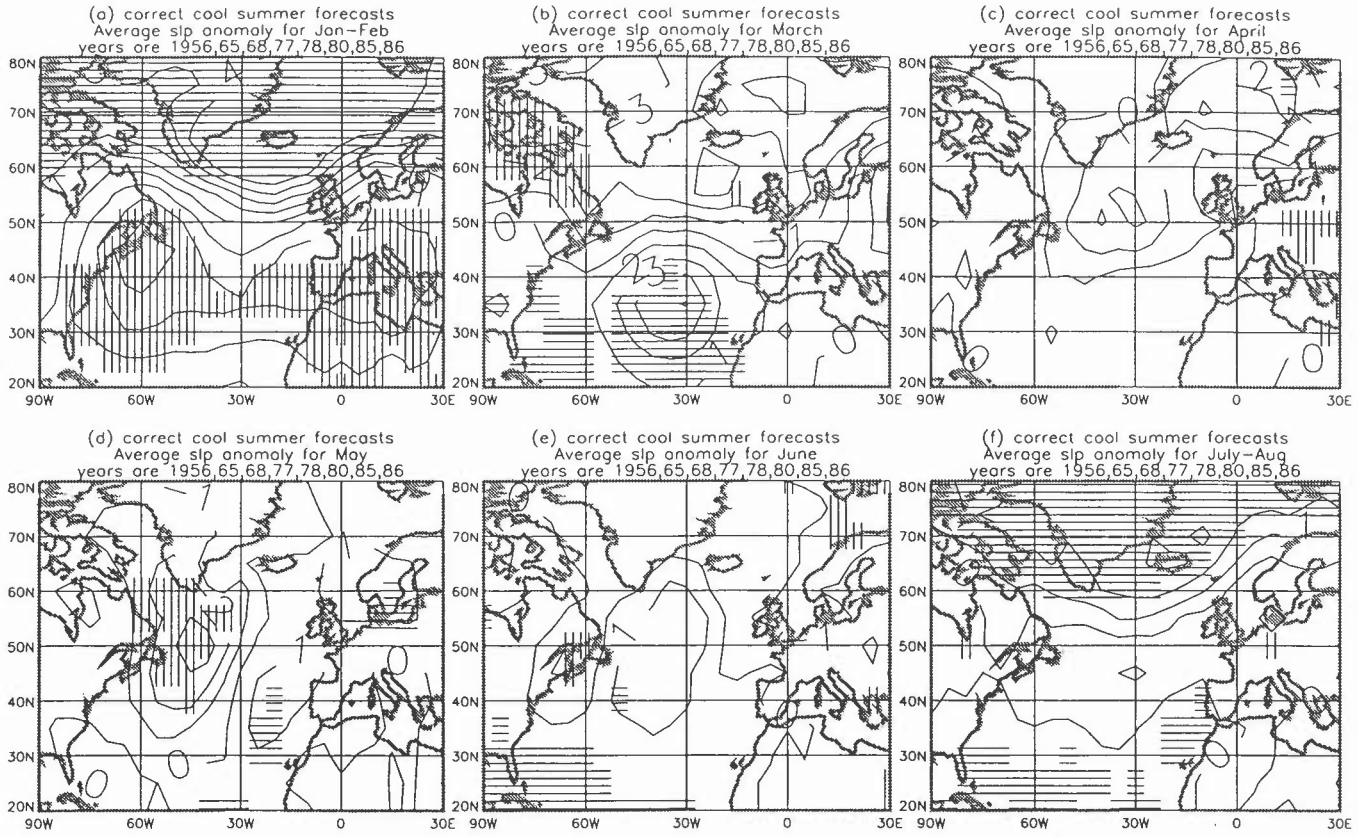

FIGURE 20

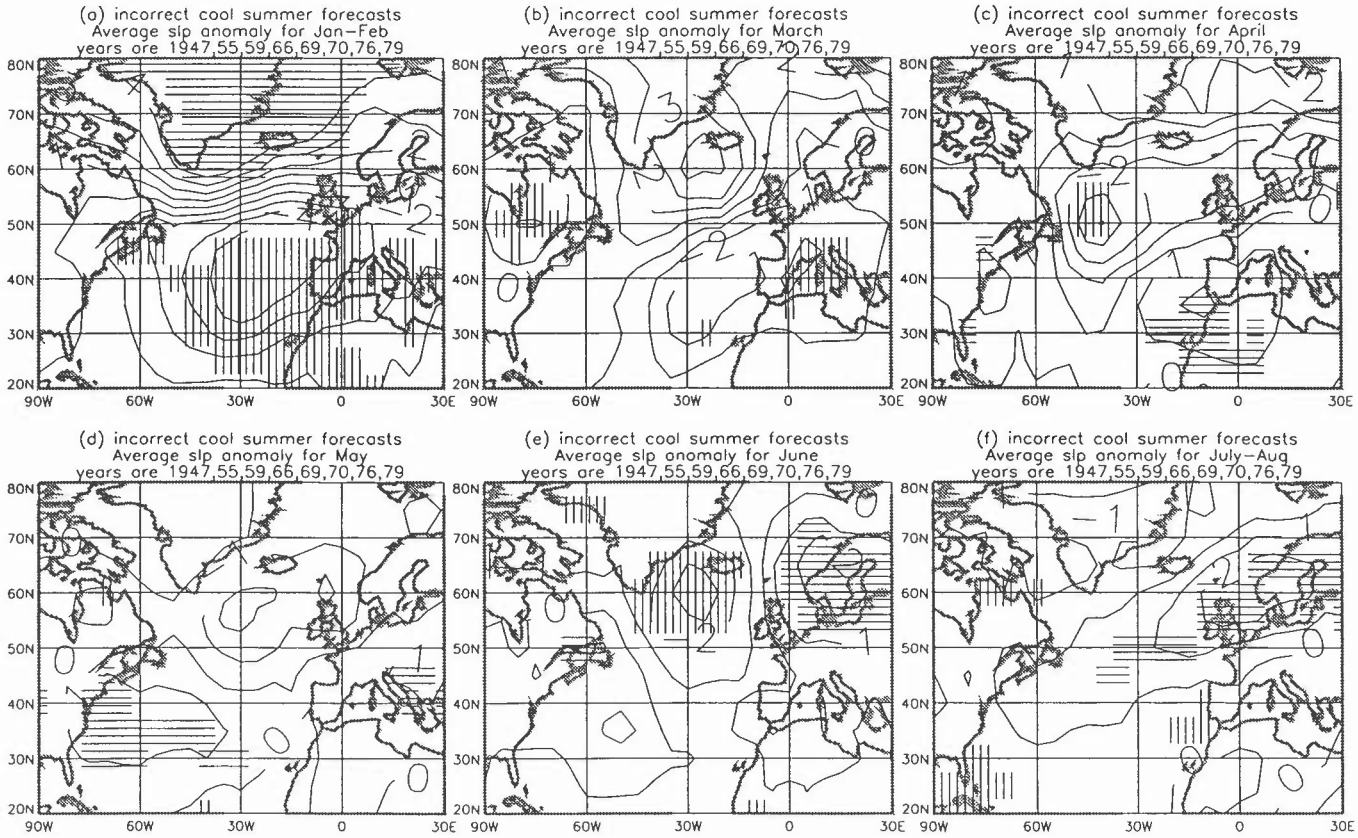

FIGURE 21

FIGURE 22

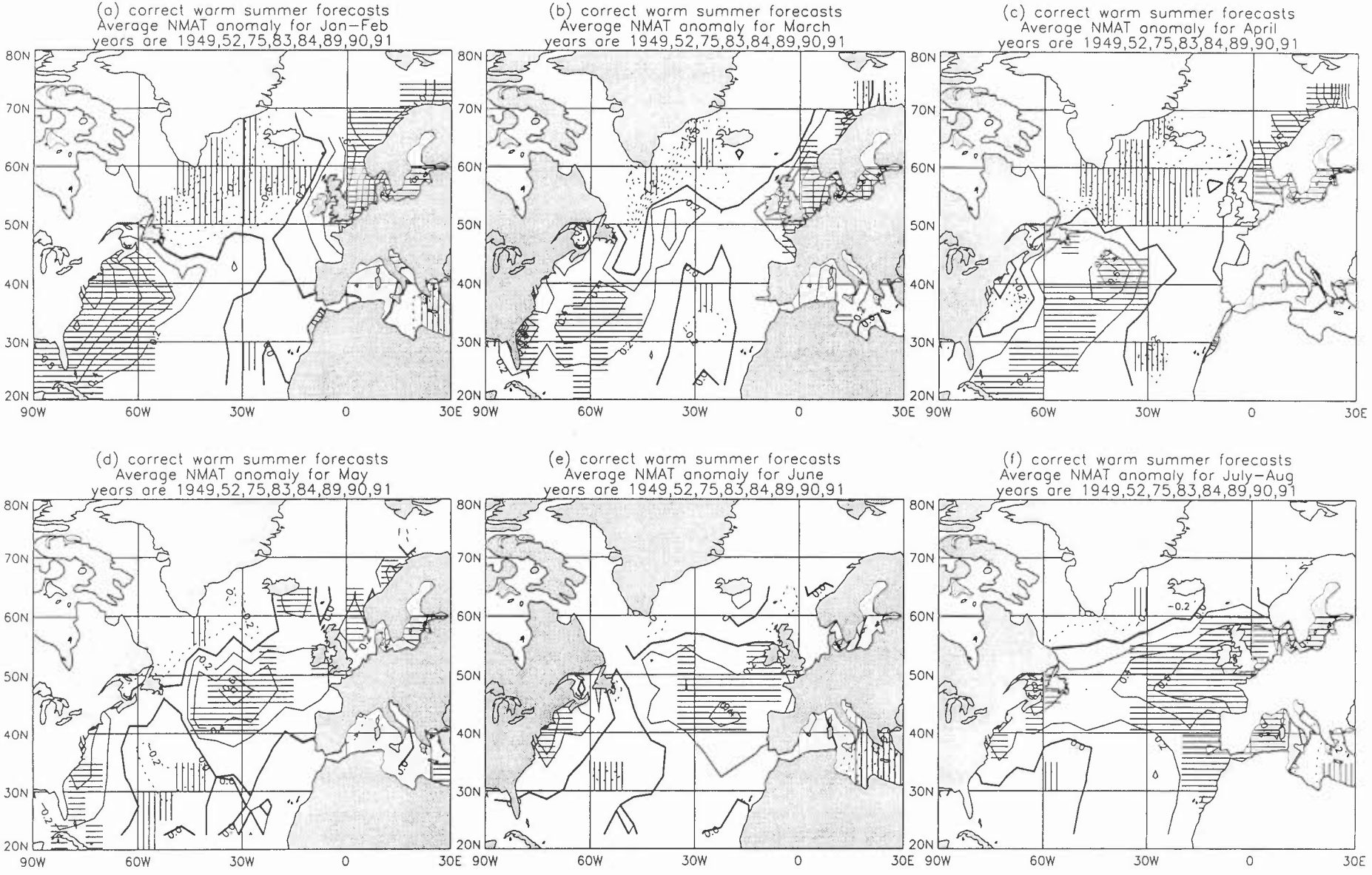
(a) correct warm summer forecasts
Average NMAT anomaly for Jan–Feb
years are 1949,52,75,83,84,89,90,91
(b) correct warm summer forecasts
Average NMAT anomaly for March
years are 1949,52,75,83,84,89,90,91
(c) correct warm summer forecasts
Average NMAT anomaly for April
years are 1949,52,75,83,84,89,90,91
(d) correct warm summer forecasts
Average NMAT anomaly for May
years are 1949,52,75,83,84,89,90,91
(e) correct warm summer forecasts
Average NMAT anomaly for June
years are 1949,52,75,83,84,89,90,91
(f) correct warm summer forecasts
Average NMAT anomaly for July–Aug
years are 1949,52,75,83,84,89,90,91
80N
70N
60N
50N
40N
30N
20N
90W
60W
30W
0
30E
-0.2

Figure 23: Squared Coherences of JF 1946–95 T1 TS with July–Aug CET